



Project No. 037005  
**CECILIA**



## **Central and Eastern Europe Climate Change Impact and Vulnerability Assessment**

Specific targeted research project  
1.1.6.3.I.3.2: Climate change impacts in central-eastern Europe

**D 5.2. Calibration of the monthly river flows over the selected period (1970- 2000) and the rainfall-runoff models according to the flood events over the same period.**

Due date of deliverable: 1<sup>st</sup> June 2007

Actual submission date: 1<sup>st</sup> June 2007

Start date of project: 1st June 2006

Duration: 36 months

Lead contractor for this deliverable: **National Institute of Hydrology and Water Management (NIHWM)**

<b>Project co-Funded by the European Commission within the Sixth Framework Programme (2002-2006)</b>		
<b>Dissemination Level</b>		
<b>PU</b>	Public	<b>X</b>
<b>PP</b>	Restricted to other programme participants (including the Commission Services)	
<b>RE</b>	Restricted to a group specified by the consortium (including the Commission Services)	
<b>CO</b>	Confidential, only for members of the consortium (including the Commission Services)	



# Calibration of the monthly river flows over the selected period (1970- 2000) and the rainfall-runoff models according to the flood events over the same period.

This deliverable provide the research of WP5 partners (CHMI, IAP, FRI and NIHW), concerning the parameters calibration of the models which will be use by each partners for assessment of climate change impacts on hydrology and water management in different river basins.

## 1. Dyje river basin (Czech Republic)

### 1.1. Calibration of the BILAN model for Dyje river basin

Because application of BILAN water balance model is suitable for catchment areas from 100 km<sup>2</sup> to approximately 1000 km<sup>2</sup>, the model will be used for assessment of these parts of Dyje river basin:

- Jevišovka river basin to the gaugestation Božice (catchment area 647 km<sup>2</sup>)
- Rokytná river basin to the cross-station Moravský Krumlov (catchment area 563 km<sup>2</sup>)
- Jihlava river basin to the gaugestation Ptáčov (catchment area 964 km<sup>2</sup>) and Mohelno (catchment area 1155 km<sup>2</sup>) and according to possibilities of the model to cross-station Ivančice (catchment area 1155 km<sup>2</sup>) besides
- Svatka river basin to the gaugestation Dalečín (catchment area 367 km<sup>2</sup>) and Vír (catchment area 487 km<sup>2</sup>) and according to possibilities of the model again to the cross-station Veverská Bítýška (catchment area 1480 km<sup>2</sup>) or Brno-Poříčí (catchment area 1640 km<sup>2</sup>) and maybe Židlochovice (with catchment area 3940 km<sup>2</sup>) besides

In this case to calibration of the model over the selected period 1970-2000 monthly runoff series at the above mentioned stations will be used.

For assessment of basin air temperature and relative air humidity there will be used measured data series of air temperature and relative humidity from 16 climate stations and for assessment of basin precipitation there will be used measured data series of precipitation from these 16 climate stations too and from next 13 precipitation stations. All these stations are situated on the Czech part of Dyje river basin.

So far, only two catchments are calibrated namely Jevišovka basin and Rokytná basin. Outputs of these calibrations are introduced in further. The units of runoff in the *Tables 1.1 to 1.4* are millimeters re-counted from cubic meters per second flown off the catchment area during the given month. The divergence (*div.*) between observed and measured runoff is expressed by equation:

$$div. = 100 \cdot (RM - R) / R \quad [\%] \quad (1.1)$$

Where: *R* is observed runoff and *RM* is simulated runoff.

#### 1.1.1. Outputs of Jevišovka river basin (gaugestation Božice) calibration by the BILAN model

From the tables and graphs below (*Table 1.1, Figure 1.1*) it can be stated that the divergences between observed and simulated runoff are mostly of a high account but it doesn't matter. For simulation of runoff in the future it is important that the monthly averages of observed and simulated runoff during the long-term period correspond with one another (*Table 1.2, Figure 1.2*). So, if the divergence between the long-term averages is not significant higher than 20%, it can be claimed that the result is acceptable. In this case it means that the values of simulated runoff at December, January and October significantly vary from the observed data and so we have to consider it in the next assessment.

### 1.1.2. Outputs of the Rokytná river basin (gaugestation Moravský Krumlov) calibration by the BILAN model

Due to the specific conditions in the Rokytná basin the results of calibration are worse than results in the Jevišovka basin (Tables 1.3, 1.4; Figures 1.3, 1.4). Significantly higher divergences between the long-term averages occur here more often – in November and December and since March to May. It has to be still considering if the Rokytná river basin will be suitable for the next assessment.

Table 1.1. Comparison of observed and simulated runoff at the station Božice in monthly step  
(R – observed runoff; RM – simulated runoff)

year	month	XI	XII	I	II	III	IV	V	VI	VII	VIII	IX	X
1970	R[mm]	1,7	3,7	1,7	8,3	29,8	11,4	3,8	4,1	2,4	2,2	1,6	3,0
	RM[mm]	23,9	19,3	19,5	22,9	41,3	19,4	12,1	7,7	4,7	2,9	1,8	1,1
	div. [%]	1299	427	1080	178	39	70	215	88	96	29	14	-63
1971	R[mm]	3,1	3,2	1,5	4,5	3,5	4,3	2,1	3,1	1,1	0,7	0,5	1,5
	RM[mm]	1,9	2,7	5,8	6,4	9,8	6,3	3,9	2,6	1,4	0,9	0,5	0,3
	div. [%]	-39,3	-15,9	279,9	44,1	179,2	47,4	84,5	-17,4	27,1	28,2	-1,0	-77,5
1972	R[mm]	1,6	1,7	1,7	3,6	3,2	6,1	11,6	4,9	2,3	2,5	0,7	1,6
	RM[mm]	0,2	0,2	0,4	14,8	2,5	3,4	4,3	1,4	0,9	0,3	0,1	0,1
	div. [%]	-87	-90	-77	316	-22	-44	-63	-72	-61	-89	-79	-94
1973	R[mm]	1,7	2,8	0,9	1,6	1,8	1,5	1,3	0,5	0,5	0,3	0,3	0,6
	RM[mm]	0,1	0,0	0,0	0,0	0,0	0,4	0,1	0,1	0,0	0,0	0,0	0,0
	div. [%]	-97	-99	-98	-99	-99	-76	-95	-88	-97	-100	-100	-100
1974	R[mm]	1,1	1,1	2,5	1,4	1,0	0,3	0,3	0,8	1,8	0,6	0,4	1,3
	RM[mm]	0,0	0,0	0,0	0,0	0,0	0,0	0,1	0,0	0,0	0,0	0,0	0,0
	div. [%]	-100	-100	-100	-97	-100	-95	-69	-95	-99	-100	-100	-100
1975	R[mm]	1,2	3,7	2,1	1,5	1,8	1,5	1,0	1,3	1,6	0,8	0,8	1,4
	RM[mm]	0,2	7,5	4,8	3,0	7,5	2,0	1,8	1,8	1,3	0,9	0,2	0,2
	div. [%]	-82	104	132	98	306	39	88	35	-21	8	-75	-86
1976	R[mm]	1,2	1,6	9,0	4,0	5,6	2,3	1,2	0,7	0,3	0,5	0,4	1,9
	RM[mm]	0,3	0,0	16,8	4,1	4,9	3,4	2,2	1,2	0,7	0,5	0,3	0,2
	div. [%]	-77	-97	88	3	-12	49	88	78	173	-8	-25	-90
1977	R[mm]	3,7	3,0	2,8	41,0	15,8	10,9	3,1	1,9	0,9	1,4	0,9	2,0
	RM[mm]	4,8	3,6	10,8	56,3	17,2	10,8	6,4	4,0	2,5	1,5	1,0	0,6
	div. [%]	32	21	291	37	9	0	108	112	189	8	4	-70
1978	R[mm]	1,5	1,4	1,4	2,1	5,4	2,2	2,4	0,8	0,5	0,1	0,1	0,6
	RM[mm]	0,4	0,2	0,1	0,1	0,1	0,2	0,4	0,0	0,0	0,0	0,0	0,0
	div. [%]	-76	-84	-90	-96	-99	-89	-84	-95	-97	-95	-97	-100
1979	R[mm]	0,6	0,7	0,7	4,1	14,3	5,0	2,0	0,9	0,7	0,8	0,7	2,3
	RM[mm]	0,0	0,0	0,0	1,4	10,4	4,7	1,8	1,3	0,7	0,4	0,3	0,2
	div. [%]	-100	-100	-100	-66	-27	-6	-9	37	1	-44	-59	-93
1980	R[mm]	2,8	4,4	2,7	6,9	3,3	7,9	4,4	3,1	1,4	0,5	0,3	3,4
	RM[mm]	6,2	13,4	9,6	8,1	5,2	4,4	2,7	1,8	0,9	0,5	0,3	0,2
	div. [%]	123	206	250	17	59	-44	-38	-41	-32	-2	-13	-95
1981	R[mm]	2,8	3,3	2,6	2,8	6,0	2,7	2,4	0,6	1,0	0,2	0,5	8,4
	RM[mm]	3,5	2,7	3,7	3,7	2,3	1,5	1,4	0,7	0,4	0,2	4,9	10,4
	div. [%]	24	-17	44	31	-62	-45	-41	2	-61	0	829	23
1982	R[mm]	4,1	2,6	6,7	9,7	11,9	5,3	3,2	2,1	4,6	5,1	1,5	3,4
	RM[mm]	5,8	6,1	10,4	10,7	6,7	4,3	3,2	2,0	1,1	0,6	0,4	0,2
	div. [%]	44	135	56	11	-44	-20	0	-5	-76	-87	-74	-93
1983	R[mm]	2,2	3,1	3,9	3,3	7,9	6,2	2,9	1,5	0,5	0,2	0,2	0,7
	RM[mm]	0,2	0,2	0,2	2,0	3,9	4,1	2,4	1,5	0,6	0,4	0,2	0,1
	div. [%]	-92	-93	-94	-39	-50	-34	-20	-4	25	101	6	-81

<b>year</b>	<b>month</b>	<b>XI</b>	<b>XII</b>	<b>I</b>	<b>II</b>	<b>III</b>	<b>IV</b>	<b>V</b>	<b>VI</b>	<b>VII</b>	<b>VIII</b>	<b>IX</b>	<b>X</b>
1984	<b>R[mm]</b>	0,8	0,9	0,8	3,0	4,8	3,4	5,1	2,4	1,1	0,9	1,5	2,4
	<b>RM[mm]</b>	0,1	0,1	0,0	0,5	1,1	2,6	4,9	1,5	0,5	0,1	0,1	0,2
	<b>div. [%]</b>	-89	-94	-96	-82	-78	-26	-2	-35	-52	-85	-94	-92
1985	<b>R[mm]</b>	2,3	2,0	1,3	9,1	16,0	7,3	6,7	4,5	1,5	9,8	2,5	2,4
	<b>RM[mm]</b>	0,3	0,9	3,1	6,3	25,7	7,4	5,5	3,1	2,0	1,3	0,8	0,4
	<b>div. [%]</b>	-86	-56	148	-32	61	1	-17	-31	36	-87	-69	-82
1986	<b>R[mm]</b>	4,4	11,1	12,6	6,5	15,3	6,4	2,3	11,3	4,5	4,2	2,1	3,4
	<b>RM[mm]</b>	3,8	24,7	9,2	10,3	8,6	5,5	3,9	2,7	1,6	0,9	0,5	0,3
	<b>div. [%]</b>	-14	122	-27	59	-44	-14	65	-76	-64	-78	-76	-91
1987	<b>R[mm]</b>	3,4	3,0	5,2	17,9	15,0	9,4	10,4	11,0	7,1	2,8	1,6	3,1
	<b>RM[mm]</b>	0,2	0,1	2,0	9,1	13,0	8,1	9,9	7,2	4,8	1,5	0,8	0,5
	<b>div. [%]</b>	-94	-96	-62	-49	-14	-14	-5	-35	-33	-46	-48	-84
1988	<b>R[mm]</b>	3,7	4,0	3,7	4,0	8,3	4,9	1,0	1,7	0,9	0,5	0,9	1,8
	<b>RM[mm]</b>	0,3	0,2	0,3	2,0	1,4	0,7	0,5	0,3	0,2	0,1	0,1	0,0
	<b>div. [%]</b>	-92	-94	-92	-51	-83	-85	-49	-80	-79	-80	-93	-98
1989	<b>R[mm]</b>	2,5	4,4	3,4	2,3	2,0	0,8	2,9	0,9	0,5	0,5	0,5	1,0
	<b>RM[mm]</b>	0,0	0,0	0,0	0,0	0,0	1,0	0,3	0,2	0,0	0,0	0,0	0,0
	<b>div. [%]</b>	-99	-99	-100	-100	-98	28	-91	-76	-96	-99	-100	-100
1990	<b>R[mm]</b>	1,1	1,0	1,0	1,2	1,5	1,3	1,1	0,5	0,4	0,2	0,3	0,7
	<b>RM[mm]</b>	0,0	0,0	0,0	0,0	0,1	0,5	0,3	0,1	0,0	0,0	0,0	0,0
	<b>div. [%]</b>	-100	-100	-100	-100	-95	-62	-71	-73	-96	-100	-99	-100
1991	<b>R[mm]</b>	1,3	1,6	1,4	0,7	1,0	0,3	1,6	0,7	0,3	0,4	0,3	0,3
	<b>RM[mm]</b>	0,0	0,0	0,0	0,0	0,0	0,1	0,9	0,4	0,0	0,0	0,0	0,0
	<b>div. [%]</b>	-100	-100	-100	-100	-100	-69	-45	-46	-84	-97	-100	-100
1992	<b>R[mm]</b>	1,2	1,3	1,7	1,2	1,4	1,0	0,6	0,2	0,4	0,3	0,3	0,5
	<b>RM[mm]</b>	0,9	3,6	6,5	4,1	4,8	2,8	1,4	0,9	0,5	0,3	0,2	0,1
	<b>div. [%]</b>	-28	182	272	241	239	168	144	341	44	22	-20	-74
1993	<b>R[mm]</b>	0,8	1,0	0,9	0,7	1,9	1,2	0,4	0,3	0,3	0,3	0,5	0,4
	<b>RM[mm]</b>	1,0	3,1	6,5	5,1	3,3	2,2	1,7	1,0	0,5	0,3	0,2	0,1
	<b>div. [%]</b>	28	210	594	588	72	85	351	183	87	14	-61	-69
1994	<b>R[mm]</b>	0,3	1,3	2,6	1,5	1,5	1,7	1,9	0,5	0,5	0,3	0,3	0,2
	<b>RM[mm]</b>	2,1	11,4	7,2	4,4	2,8	4,0	5,4	0,8	0,5	0,3	0,2	0,1
	<b>div. [%]</b>	634	766	183	199	80	133	185	64	-1	-19	-39	-54
1995	<b>R[mm]</b>	1,0	0,7	0,8	0,9	1,1	0,6	0,6	1,6	0,5	0,4	1,3	2,2
	<b>RM[mm]</b>	0,1	0,1	0,0	0,0	0,4	0,8	0,9	0,8	0,1	0,1	3,6	2,4
	<b>div. [%]</b>	-93	-91	-97	-98	-59	34	65	-51	-81	-81	176	7
1996	<b>R[mm]</b>	0,8	2,1	3,5	2,5	17,1	21,8	7,5	3,2	1,4	1,3	2,1	3,9
	<b>RM[mm]</b>	1,8	4,8	12,3	14,6	11,1	7,0	7,9	6,0	2,0	1,4	0,8	0,6
	<b>div. [%]</b>	129	128	247	487	-35	-68	5	88	44	6	-64	-84
1997	<b>R[mm]</b>	3,3	2,8	2,4	6,0	6,1	5,4	4,0	1,4	16,2	4,3	2,5	3,3
	<b>RM[mm]</b>	0,4	0,2	0,4	0,7	0,9	0,7	0,9	0,3	22,7	16,1	9,3	5,8
	<b>div. [%]</b>	-87	-94	-83	-88	-85	-88	-78	-79	40	278	270	77
1998	<b>R[mm]</b>	2,2	5,8	4,4	3,2	2,9	2,8	1,5	1,1	0,3	0,3	0,7	2,1
	<b>RM[mm]</b>	5,6	16,6	10,2	6,3	4,1	2,6	1,8	1,1	0,6	0,4	0,2	0,9
	<b>div. [%]</b>	152	187	131	97	41	-7	19	0	136	9	-68	-59
1999	<b>R[mm]</b>	3,4	1,7	1,1	2,4	4,1	2,6	1,7	1,6	6,6	0,5	1,3	1,7
	<b>RM[mm]</b>	3,1	1,8	1,1	2,1	3,3	2,9	2,0	1,1	0,8	0,3	0,2	0,1
	<b>div. [%]</b>	-9	6	1	-11	-19	11	20	-32	-88	-30	-84	-93
2000	<b>R[mm]</b>	2,1	1,6	3,7	8,6	6,0	7,1	1,6	0,5	0,3	1,2	0,6	2,1
	<b>RM[mm]</b>	0,1	0,0	1,9	3,7	16,1	8,9	5,7	3,5	2,2	1,3	0,8	0,5
	<b>div. [%]</b>	-96	-97	-50	-57	167	26	250	643	621	10	31	-76

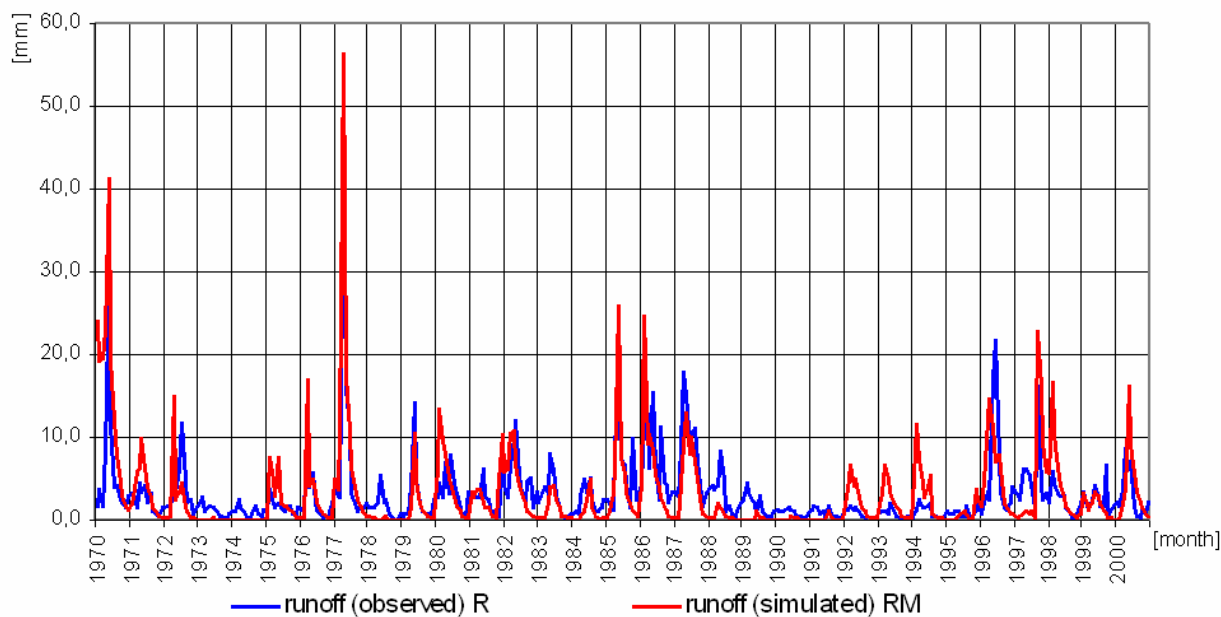


Figure 1.1. Comparison of observed and simulated runoff at the station Božice in monthly step

Table 1.2. Comparison of monthly averages of observed and simulated runoff at the station Božice during the calibrated period 1970-2000

	XI	XII	I	II	III	IV	V	VI	VII	VIII	IX	X
<b>R [mm]</b>	2,1	2,7	2,9	5,4	7,0	4,7	3,0	2,3	2,0	1,4	0,9	2,1
<b>RM [mm]</b>	2,2	4,0	4,6	6,5	6,7	4,0	3,1	1,8	1,8	1,1	0,9	0,8
<b>div. [%]</b>	4,8	48,1	58,6	20,4	-4,3	-14,9	3,3	-21,7	-10,0	-21,4	0,0	-61,9

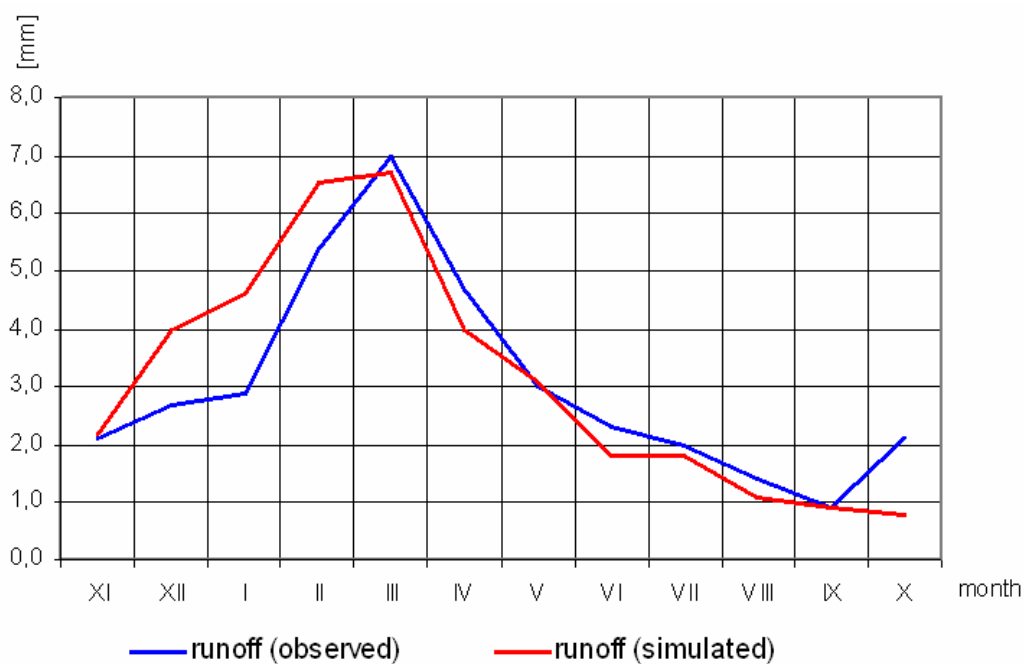


Figure 1.2. Comparison of monthly averages of observed and simulated runoff at the station Božice during the calibrated period 1970-2000

Table 1.3. Comparison of observed and simulated runoff at the station Mor. Krumlov in monthly step

year	month	XI	XII	I	II	III	IV	V	VI	VII	VIII	IX	X
1970	R[mm]	1,7	3,7	1,7	8,3	29,8	11,4	3,8	4,1	2,4	2,2	1,6	3,0
	RM[mm]	11,6	4,7	6,2	7,2	71,8	2,4	2,2	2,2	1,8	1,7	1,6	1,5
	div. [%]	581,7	27,5	276,7	-13,0	141,1	-78,6	-42,5	-46,7	-23,8	-23,6	2,0	-48,7
1971	R[mm]	3,1	3,2	1,5	4,5	3,5	4,3	2,1	3,1	1,1	0,7	0,5	1,5
	RM[mm]	5,2	7,8	5,5	5,6	11,7	2,4	2,5	2,3	1,7	1,6	1,6	1,5
	div. [%]	65,5	140,9	257,9	24,7	235,6	-43,4	17,0	-27,7	53,6	140,4	188,7	2,2
1972	R[mm]	1,6	1,7	1,7	3,6	3,2	6,1	11,6	4,9	2,3	2,5	0,7	1,6
	RM[mm]	1,5	1,5	1,4	17,6	1,4	3,2	5,5	2,0	1,6	1,2	1,1	1,0
	div. [%]	-7	-15	-18	395	-56	-48	-53	-59	-29	-54	53	-35
1973	R[mm]	1,7	2,8	0,9	1,6	1,8	1,5	1,3	0,5	0,5	0,3	0,3	0,6
	RM[mm]	1,0	1,0	0,9	0,9	0,9	1,4	0,9	0,9	0,8	0,8	0,7	0,7
	div. [%]	-39,8	-64,9	4,8	-41,8	-50,0	-6,0	-27,6	79,3	56,2	150,0	177,3	9,1
1974	R[mm]	1,1	1,1	2,5	1,4	1,0	0,3	0,3	0,8	1,8	0,6	0,4	1,3
	RM[mm]	0,7	0,7	0,6	0,7	0,6	0,6	0,7	0,6	0,6	0,5	0,5	0,5
	div. [%]	-35,2	-39,4	-74,7	-50,9	-36,0	103,7	139,8	-25,3	-68,2	-15,8	28,3	-61,5
1975	R[mm]	1,2	3,7	2,1	1,5	1,8	1,5	1,0	1,3	1,6	0,8	0,8	1,4
	RM[mm]	2,4	22,2	2,7	1,0	12,6	1,0	1,6	1,6	1,0	0,9	0,8	0,8
	div. [%]	95,7	501,1	28,9	-34,5	586,8	-29,5	63,1	27,1	-39,2	10,7	-3,3	-42,6
1976	R[mm]	1,2	1,6	9,0	4,0	5,6	2,3	1,2	0,7	0,3	0,5	0,4	1,9
	RM[mm]	0,9	0,7	4,0	7,4	2,2	1,1	1,3	0,8	0,8	0,8	0,8	0,7
	div. [%]	-26,7	-55,4	-55,7	84,6	-60,8	-50,8	10,1	26,4	197,9	55,3	96,7	-60,7
1977	R[mm]	3,7	3,0	2,8	41,0	15,8	10,9	3,1	1,9	0,9	1,4	0,9	2,0
	RM[mm]	7,5	5,5	6,9	78,4	4,8	1,8	1,3	1,1	1,0	1,0	0,9	0,9
	div. [%]	104,7	84,9	149,9	91,2	-69,4	-83,1	-57,6	-42,8	17,4	-32,3	0,9	-55,4
1978	R[mm]	1,5	1,4	1,4	2,1	5,4	2,2	2,4	0,8	0,5	0,1	0,1	0,6
	RM[mm]	0,9	0,8	0,8	0,8	0,8	1,4	1,6	0,9	0,7	0,7	0,6	0,6
	div. [%]	-43,8	-40,1	-43,5	-62,5	-86,0	-34,0	-35,5	24,6	57,6	468,8	482,1	-4,0
1979	R[mm]	0,6	0,7	0,7	4,1	14,3	5,0	2,0	0,9	0,7	0,8	0,7	2,3
	RM[mm]	0,6	0,6	0,6	0,5	29,2	2,3	0,6	0,8	0,5	0,5	0,4	0,4
	div. [%]	5,5	-20,2	-16,2	-86,9	105,0	-54,8	-71,7	-13,2	-27,3	-40,6	-34,2	-82,1
1980	R[mm]	2,8	4,4	2,7	6,9	3,3	7,9	4,4	3,1	1,4	0,5	0,3	3,4
	RM[mm]	8,2	16,9	4,2	5,8	1,2	2,4	2,1	1,3	1,0	0,8	0,8	0,8
	div. [%]	195,2	284,1	55,2	-16,2	-62,3	-69,7	-52,8	-58,8	-26,9	75,4	145,6	-77,1
1981	R[mm]	2,8	3,3	2,6	2,8	6,0	2,7	2,4	0,6	1,0	0,2	0,5	8,4
	RM[mm]	7,1	8,2	5,5	4,3	1,2	1,2	1,5	1,2	1,1	1,0	5,2	21,6
	div. [%]	152,4	148,0	111,5	53,3	-80,4	-54,4	-39,4	95,4	11,9	373,4	889,5	156,8
1982	R[mm]	4,1	2,6	6,7	9,7	11,9	5,3	3,2	2,1	4,6	5,1	1,5	3,4
	RM[mm]	3,3	7,2	3,9	7,5	20,3	1,7	2,3	1,9	1,6	1,5	1,4	1,4
	div. [%]	-18,7	176,5	-41,1	-23,1	71,4	-68,1	-27,5	-10,7	-65,7	-71,1	-8,2	-60,2
1983	R[mm]	2,2	3,1	3,9	3,3	7,9	6,2	2,9	1,5	0,5	0,2	0,2	0,7
	RM[mm]	1,3	1,4	2,8	6,3	1,3	2,9	2,1	1,7	1,2	1,1	1,1	1,1
	div. [%]	-39,9	-54,7	-26,7	93,7	-83,3	-53,0	-27,5	12,9	145,8	513,0	403,2	42,0
1984	R[mm]	0,8	0,9	0,8	3,0	4,8	3,4	5,1	2,4	1,1	0,9	1,5	2,4
	RM[mm]	1,0	1,0	1,0	0,9	2,9	3,2	4,1	1,3	1,0	0,8	0,8	1,0
	div. [%]	29,9	13,5	13,3	-68,9	-39,5	-7,2	-18,0	-45,0	-6,6	-13,0	-49,8	-60,3

year	month	XI	XII	I	II	III	IV	V	VI	VII	VIII	IX	X
1985	R[mm]	2,3	2,0	1,3	9,1	16,0	7,3	6,7	4,5	1,5	9,8	2,5	2,4
	RM[mm]	2,8	7,5	0,9	3,6	55,3	1,0	3,0	1,9	1,6	5,2	1,0	0,8
	div. [%]	19,9	267,1	-29,5	-60,3	245,9	-86,1	-55,9	-57,1	7,7	-47,6	-60,2	-66,3
1986	R[mm]	4,4	11,1	12,6	6,5	15,3	6,4	2,3	11,3	4,5	4,2	2,1	3,4
	RM[mm]	16,4	16,8	7,8	2,8	20,0	1,6	2,2	2,0	1,6	1,4	1,3	1,3
	div. [%]	269,2	50,8	-37,6	-56,6	30,3	-74,8	-7,8	-82,4	-65,7	-67,0	-38,0	-63,3
1987	R[mm]	3,4	3,0	5,2	17,9	15,0	9,4	10,4	11,0	7,1	2,8	1,6	3,1
	RM[mm]	1,2	1,2	1,1	1,1	6,5	1,2	8,1	9,8	4,7	1,6	1,2	1,0
	div. [%]	-64,2	-60,5	-78,0	-93,8	-56,8	-87,3	-22,5	-10,7	-34,1	-44,5	-23,8	-66,7
1988	R[mm]	3,7	4,0	3,7	4,0	8,3	4,9	1,0	1,7	0,9	0,5	0,9	1,8
	RM[mm]	1,0	1,1	2,7	11,3	3,1	1,3	1,2	1,1	1,0	1,0	1,0	0,9
	div. [%]	-73,5	-73,4	-27,0	179,3	-62,6	-74,2	17,2	-35,6	21,2	100,9	7,0	-49,7
1989	R[mm]	2,5	4,4	3,4	2,3	2,0	0,8	2,9	0,9	0,5	0,5	0,5	1,0
	RM[mm]	0,9	0,9	0,8	0,8	0,9	2,2	1,6	1,1	0,7	0,7	0,7	0,6
	div. [%]	-63,5	-80,3	-75,0	-65,1	-57,4	174,9	-47,2	15,2	41,4	44,4	19,1	-39,3
1990	R[mm]	1,1	1,0	1,0	1,2	1,5	1,3	1,1	0,5	0,4	0,2	0,3	0,7
	RM[mm]	0,6	0,6	0,6	0,6	0,6	1,4	0,8	0,6	0,5	0,5	0,4	0,4
	div. [%]	-45,9	-43,3	-40,0	-55,5	-59,7	6,0	-22,8	16,9	19,5	113,6	66,0	-36,5
1991	R[mm]	1,3	1,6	1,4	0,7	1,0	0,3	1,6	0,7	0,3	0,4	0,3	0,3
	RM[mm]	0,4	0,4	0,4	0,4	0,4	0,5	1,6	1,0	0,4	0,3	0,3	0,3
	div. [%]	-66,8	-74,9	-72,1	-46,2	-63,4	61,9	-1,8	35,1	41,0	-18,5	-1,3	-4,7
1992	R[mm]	1,2	1,3	1,7	1,2	1,4	1,0	0,6	0,2	0,4	0,3	0,3	0,5
	RM[mm]	5,7	6,7	10,0	0,6	7,2	1,1	0,7	0,7	0,6	0,6	0,5	0,5
	div. [%]	367,6	415,9	473,2	-49,9	410,4	10,1	15,3	217,6	55,6	105,7	108,4	7,5
1993	R[mm]	0,8	1,0	0,9	0,7	1,9	1,2	0,4	0,3	0,3	0,3	0,5	0,4
	RM[mm]	1,0	6,7	7,3	0,8	0,8	0,8	1,0	0,8	0,7	0,7	0,7	0,6
	div. [%]	25,4	557,5	673,9	9,4	-59,4	-30,7	158,8	151,1	155,5	139,9	28,8	57,3
1994	R[mm]	0,3	1,3	2,6	1,5	1,5	1,7	1,9	0,5	0,5	0,3	0,3	0,2
	RM[mm]	0,8	11,4	1,4	0,8	0,8	2,9	3,9	0,8	0,7	0,7	0,6	0,6
	div. [%]	182,0	764,7	-44,7	-45,9	-49,3	68,9	105,2	55,8	56,0	106,8	144,1	185,0
1995	R[mm]	1,0	0,7	0,8	0,9	1,1	0,6	0,6	1,6	0,5	0,4	1,3	2,2
	RM[mm]	0,6	0,7	0,6	0,5	1,2	1,6	1,4	1,2	0,6	0,6	3,6	0,5
	div. [%]	-36,9	-3,8	-28,6	-38,0	11,0	174,9	154,3	-24,7	16,2	38,5	178,2	-76,8
1996	R[mm]	0,8	2,1	3,5	2,5	17,1	21,8	7,5	3,2	1,4	1,3	2,1	3,9
	RM[mm]	0,8	4,4	4,2	3,9	8,4	18,2	4,6	4,7	1,4	1,2	0,9	0,9
	div. [%]	-0,7	110,6	18,1	58,0	-50,7	-16,4	-38,3	49,6	-0,3	-6,5	-57,7	-77,5
1997	R[mm]	3,3	2,8	2,4	6,0	6,1	5,4	4,0	1,4	16,2	4,3	2,5	3,3
	RM[mm]	0,9	0,7	0,7	4,2	1,1	1,0	1,2	0,8	28,0	3,0	1,2	1,2
	div. [%]	-73,6	-75,1	-71,6	-30,1	-81,6	-82,2	-69,6	-40,5	73,1	-28,9	-51,2	-64,6
1998	R[mm]	2,2	5,8	4,4	3,2	2,9	2,8	1,5	1,1	0,3	0,3	0,7	2,1
	RM[mm]	5,1	21,5	1,6	1,5	1,6	1,7	1,5	1,4	1,3	1,3	1,2	11,4
	div. [%]	127,2	272,6	-63,0	-52,4	-44,4	-38,1	-0,3	33,7	410,0	270,5	66,8	454,2
1999	R[mm]	3,4	1,7	1,1	2,4	4,1	2,6	1,7	1,6	6,6	0,5	1,3	1,7
	RM[mm]	6,5	1,4	1,5	7,9	1,5	2,8	2,0	1,8	1,5	1,3	1,2	1,2
	div. [%]	90,4	-17,5	28,6	229,1	-63,7	5,9	23,6	10,6	-76,6	163,9	-2,5	-30,5
2000	R[mm]	2,1	1,6	3,7	8,6	6,0	7,1	1,6	0,5	0,3	1,2	0,6	2,1
	RM[mm]	1,2	1,1	1,8	19,5	22,6	1,5	1,6	1,4	1,3	1,3	1,2	1,2
	div. [%]	-45,4	-30,1	-50,7	127,4	274,6	-79,1	-2,3	195,9	350,8	6,0	95,9	-43,2

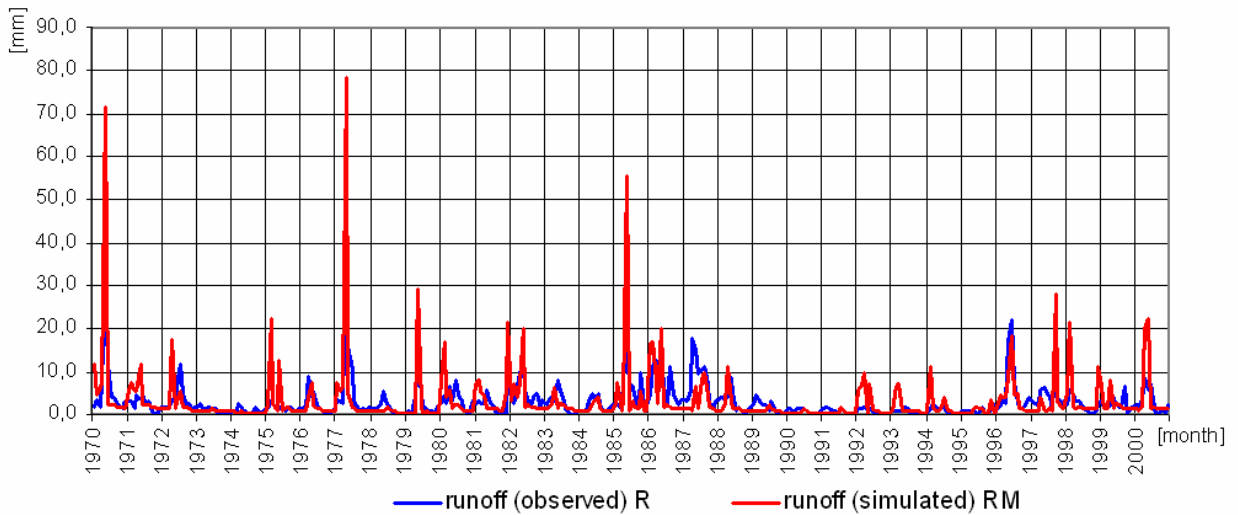


Figure 1.3. Comparison of observed and simulated runoff at the station Moravský Krumlov in monthly step

Table 1.4. Comparison of monthly averages of observed and simulated runoff at the station Moravský Krumlov during the calibrated period 1970-2000

	XI	XII	I	II	III	IV	V	VI	VII	VIII	IX	X
<b>R [mm]</b>	2,1	2,7	2,9	5,4	7,0	4,7	3,0	2,3	2,0	1,4	0,9	2,1
<b>RM [mm]</b>	3,2	5,3	2,9	6,6	9,5	2,3	2,1	1,7	2,0	1,2	1,1	1,9
<b>div. [%]</b>	52,4	96,3	0,0	22,2	35,7	-51,1	-30,0	-26,1	0,0	-14,3	22,2	-9,5

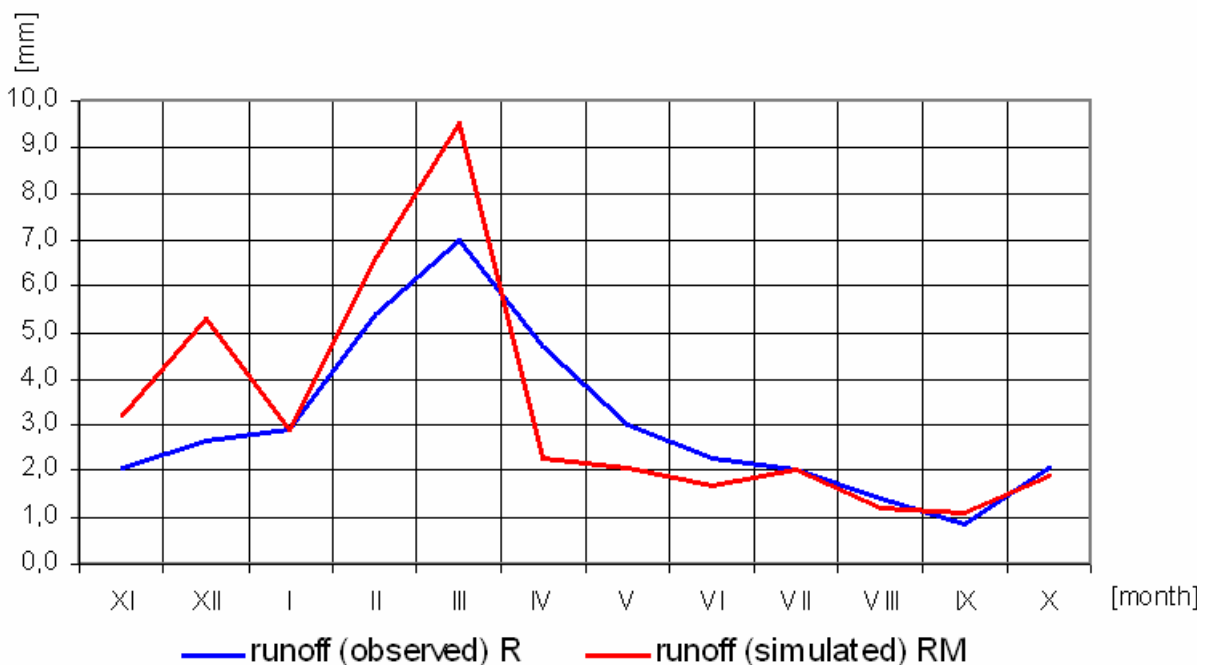


Figure 1.4. Comparison of monthly averages of observed and simulated runoff at the station Moravský Krumlov during the calibrated period 1970-2000

## 1.2. The simulation of flood events

In the Czech Republic the most of the floods are caused by precipitation and snow melting, which occurred just in the territory of this country. That's because almost all the water of Czech Republic is drained off to the other countries and only a very small amount flows in (e.g. an Austrian part of the Dyje catchment).

The hydrological model simulation of passage of floods, which occurred before 2000, is very complicated. The main problem is availability of the input data for the model. If we want to focus on the extremes, we need the data of a very high time and spatial accuracy.

Since the operative hydrological modelling in the Czech Republic has started in 1996 (in Odra river basin), the strong demands on higher concentration of a raingauge networks was given after 2000. The great improvement brought the year 2002, when the computation of the quantitative precipitation estimate (QPE) based on radar measurement combined with information from raingauges started.

### 1.2.1. The simulation of historical floods

The simulation of historical flood events is only of an informative character. Since the raingauge network was very thin before 2000, it was necessary to replace some model rainfall-areas with the near raingauges with one-hour step measurement, as it is for example depicted on *Figure 1.5*.

The selected results of the simulations are given on *Figures 1.6-1.10*. It is obvious, that the hydrological model is able to simulate the rainfall-runoff process in the catchment, but from the point of view of the hydrological extremes, it gives only partial information. E.g. the *Figure 1.6* shows the simulation in Ptáčov profile (the flood in May 1985), which is quite reliable. But the simulation of the same flood event in Oslavany profile (*Figure 1.7*) is unsuccessful taking into account the peak discharge. The similar situation is with the Bílovice profile for the floods in May 1985 and July 1997 (*Figures 1.9 and 1.10*).



*Figure 1.5. Picture shows the substitution of raingauges in Jihlava river basin for a calibration episode May 1985. The raingauges with available 1-hour precipitation data are marked by black color, while the green color marks the later established raingauges with 1 hour step measurement.*

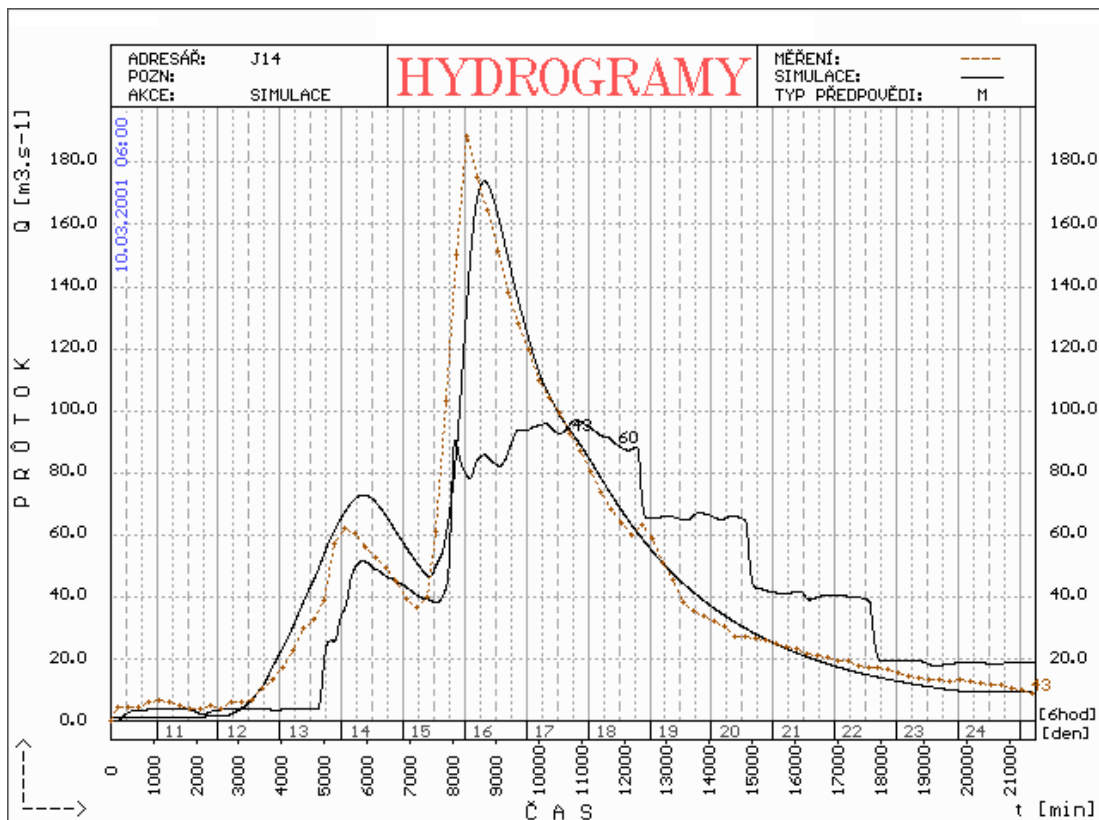


Figure 1.6. The flood event May 1985 - the simulation of discharge in Ptáčov profile (no. 43) made by HYDROG model compared with measurement (brown color). The profile no. 66 is the final profile of the model of the catchment.

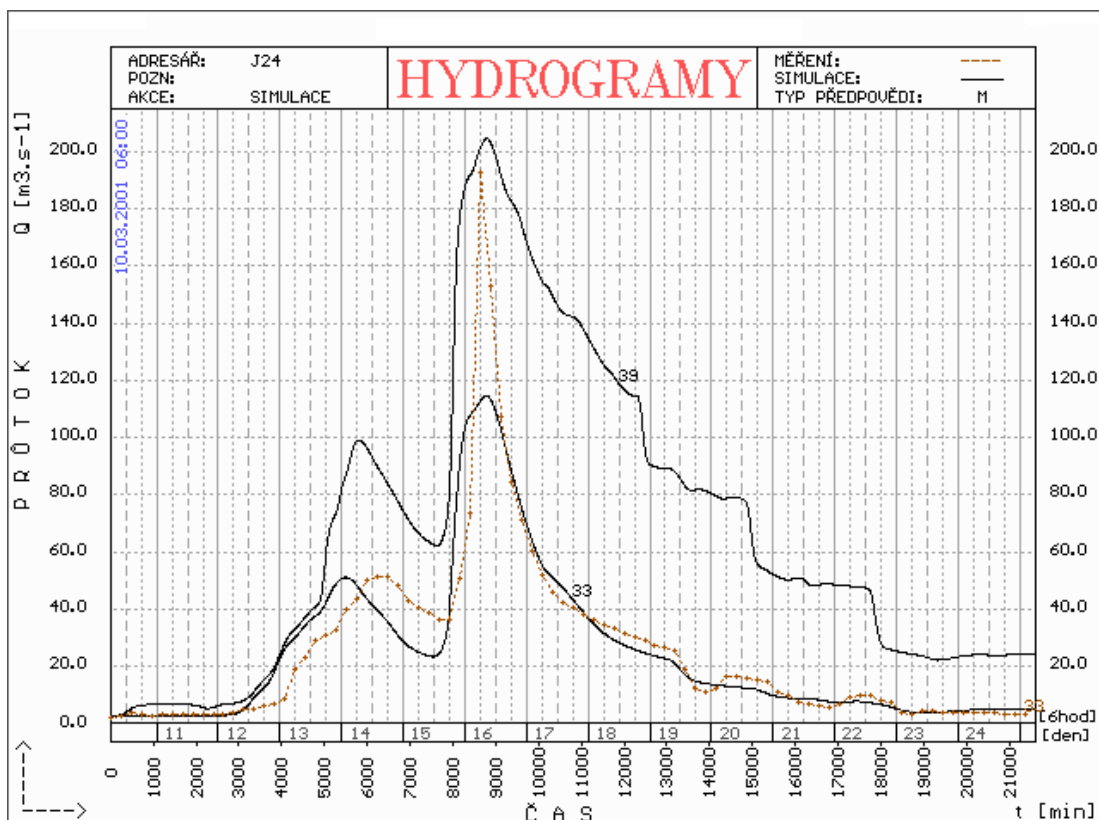


Figure 1.7. The flood event May 1985 - the simulation of discharge in Oslavany profile (no. 33) made by HYDROG model compared with measurement (brown color). The profile no. 39 is the final profile of the model of the catchment.

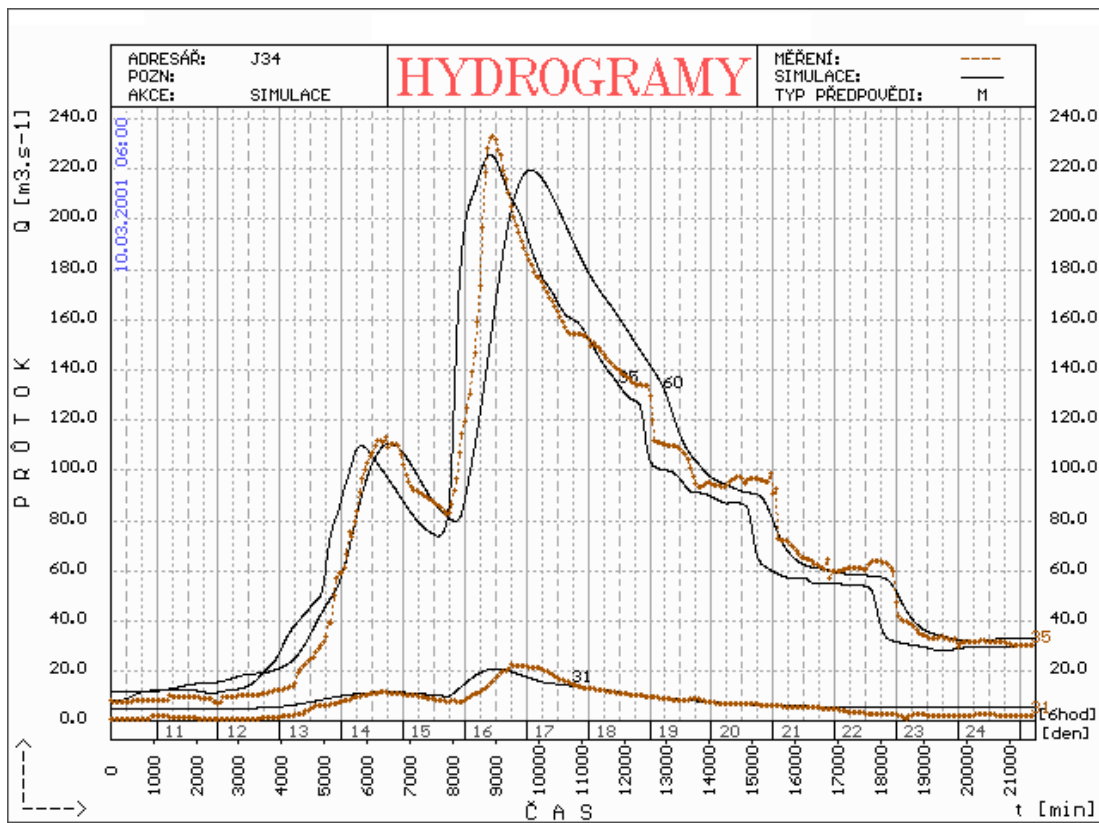


Figure 1.8. The flood event May 1985 - the simulation of discharge in Moravský Krumlov profile (no. 31) and Oslavany profile (no. 35) made by HYDROG model compared with measurement (brown color). The profile no. 60 is the final profile of the cathment model.

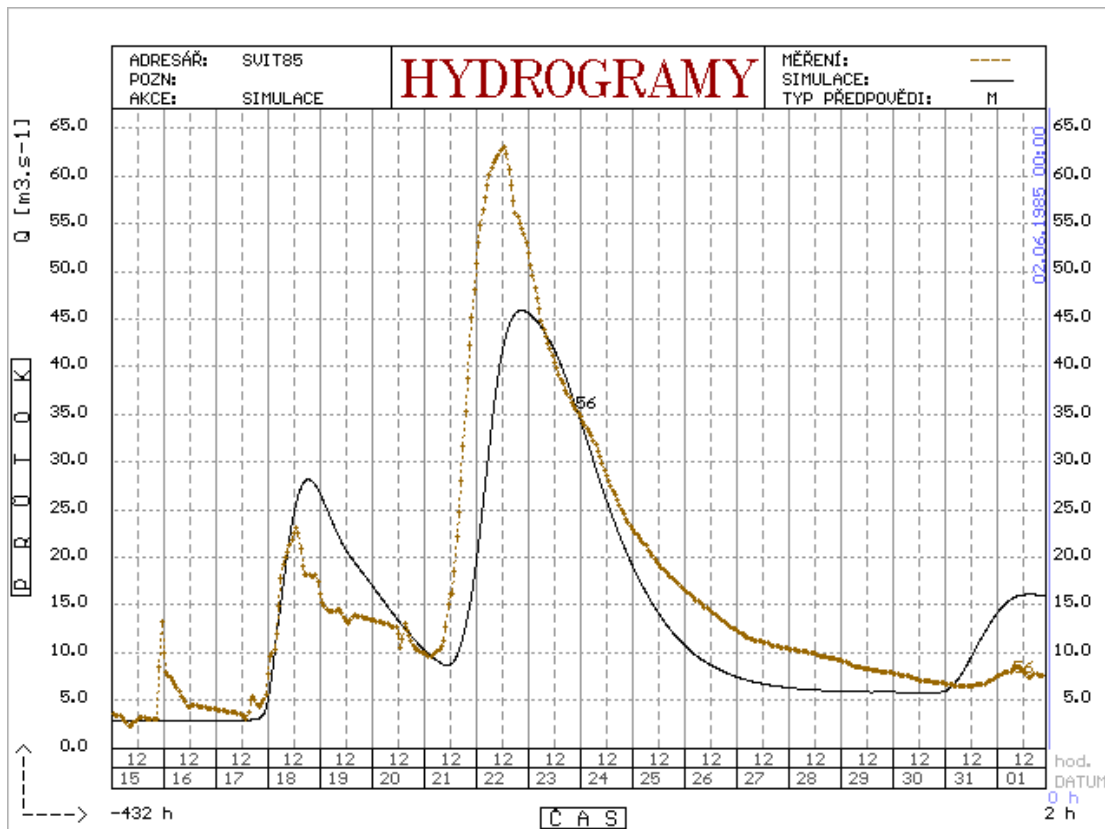


Figure 1.9. The flood event May 1985 - the simulation of discharge in Bilovice profile (no. 56) made by HYDROG model compared with measurement (brown color).

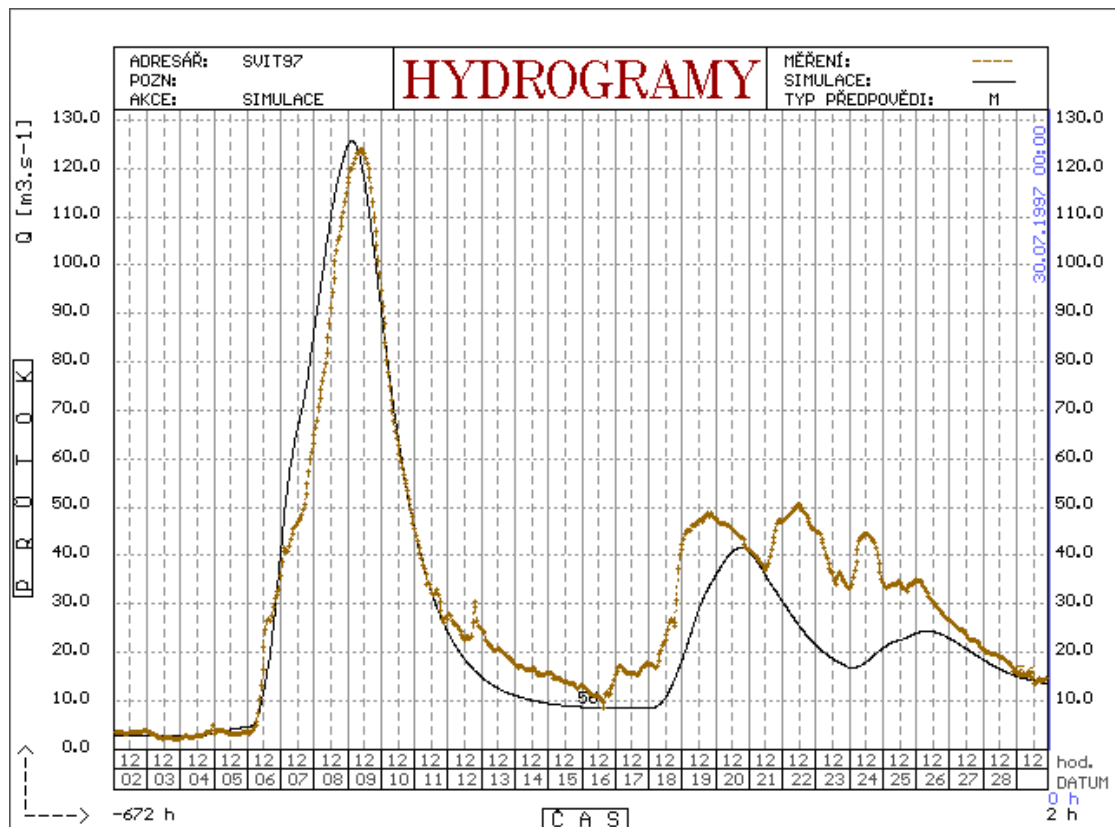


Figure 1.10. The flood event July 1997 - the simulation of discharge in Bílovice profile (no. 56) made by HYDROG model compared with measurement (brown color).

### 1.2.2. The simulation of flood events, which occurred after 2000

As it was already mentioned, it is difficult to simulate the passages of historical floods because of absence of sufficiently detail time and spatial input data. Nowadays the situation is much better. Since 2002 the quantitative precipitation estimates (QPE) are calculated every hour. These estimates are based on radar measurement combined with rain gauge measurement (see Šálek, 2004) and they are the standard input for the operative hydrological modeling (see Březková and Soukalová, 2006).

The model catchments were divided into smaller rainfall areas (average size about 90 km<sup>2</sup> – see Figure 1.11) which enables better to describe the rainfall process, e.g. the more accurate input rainfall data for the model. For the simulation of the floods the continuous database of QPE for model rainfall areas was created. This database stores the data since 2002 and performs the very good estimation of the real precipitation – a proper input for HYDROG model. For the better evaluation of the hydrological model initial conditions the Matlab software was used.

The results of simulations of floods in August 2002, March 2005, March-April 2006 and July 2006 are given on Figures 1.12 to 1.15. The correspondence of the simulated and real discharges is good – much better than simulation of historical floods. The worst result gives the simulation of the flood in Podhradí in June 2006. This flood event is quite atypical – it represents the large-scaled flash flood which caused the record peak discharge in Podhradí profile in history of measurement.

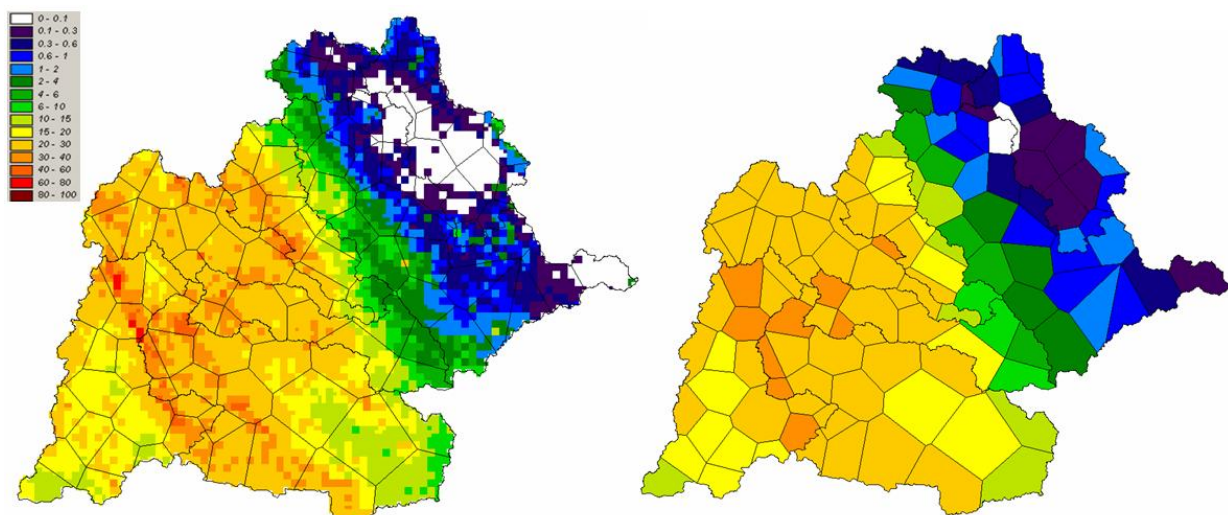


Figure 1.11. The simplification of rainfall in the HYDROG model. Left – the radar QPE (in mm), right – model input. The total size of the catchment is about 11600 km<sup>2</sup>, catchment is divided into 127 segments, where the rainfall is for a given time-step considered as a constant value.

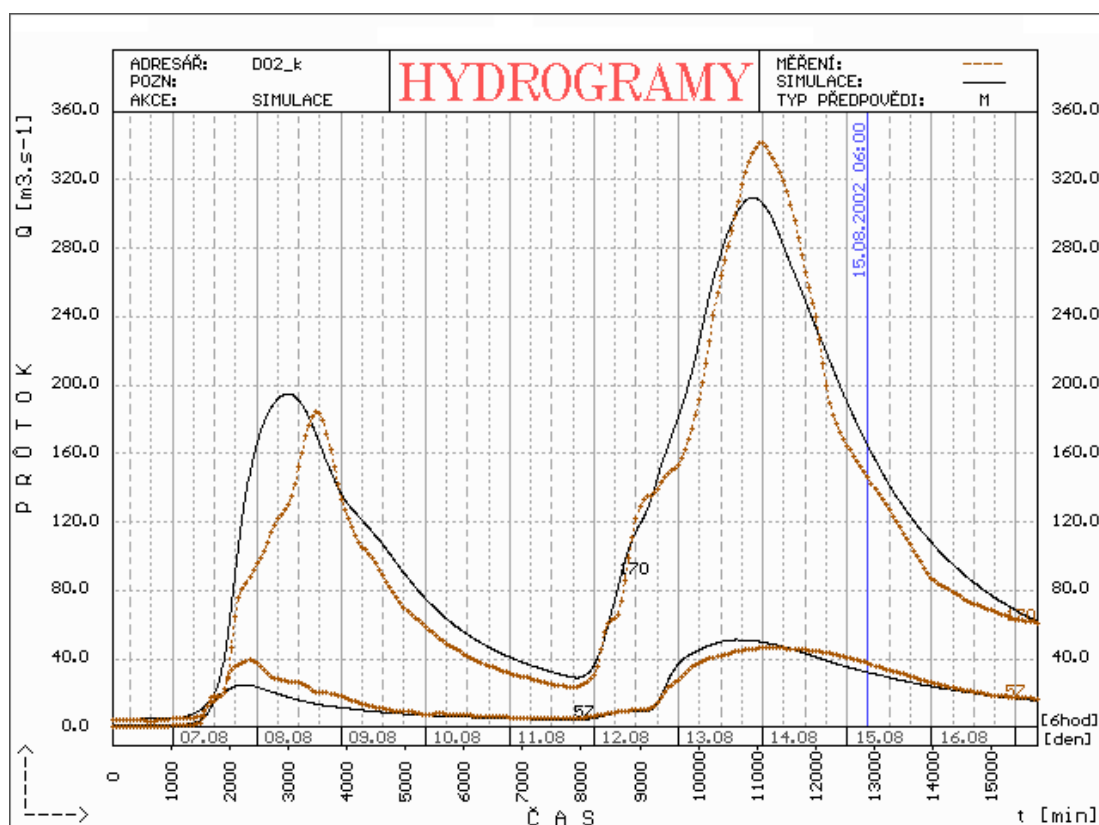


Figure 1.12. The flood event August 2002 - the simulation of discharge in Janov profile (no. 57) and Podhradí profile (no. 170) made by HYDROG model compared with measurement (brown color).

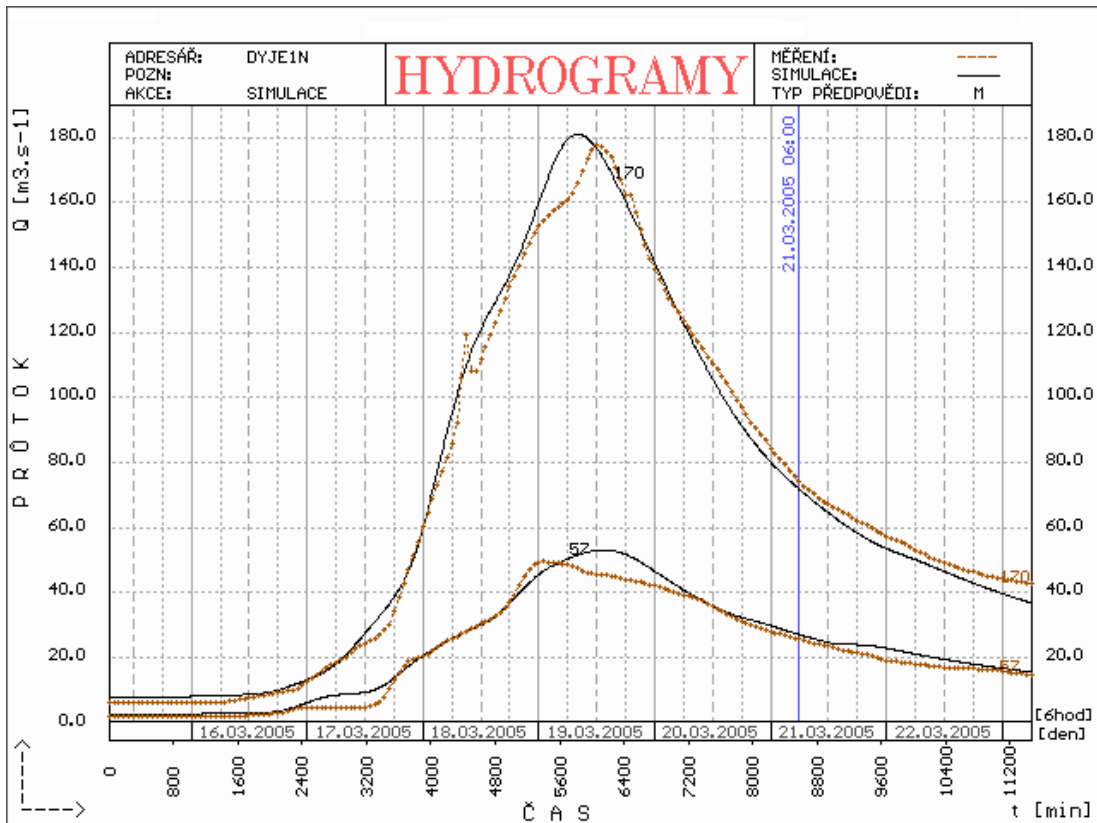


Figure 1.13. The flood event March 2005 - the simulation of discharge in Janov profile (no. 57) and Podhradí profile (no. 170) made by HYDROG model compared with measurement (brown color).

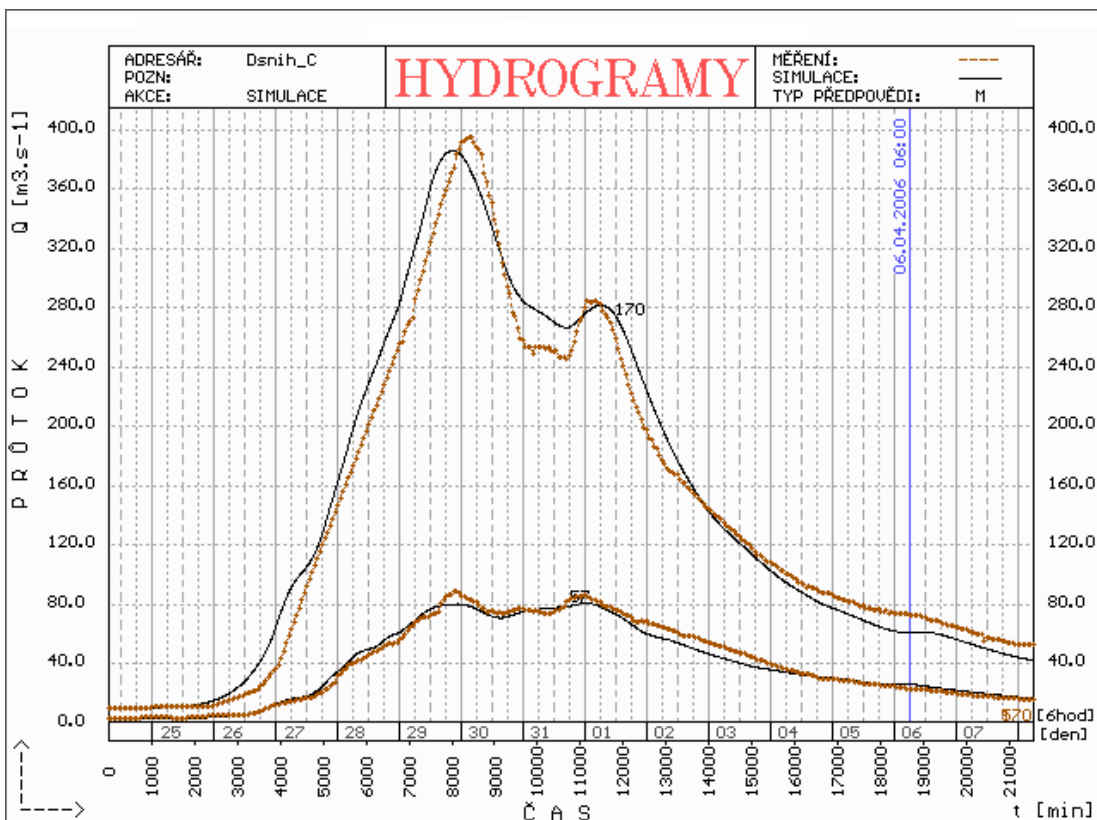


Figure 1.14. The flood event March-April 2006 - the simulation of discharge in Janov profile (no. 57) and Podhradí profile (no. 170) made by HYDROG model compared with measurement (brown color).

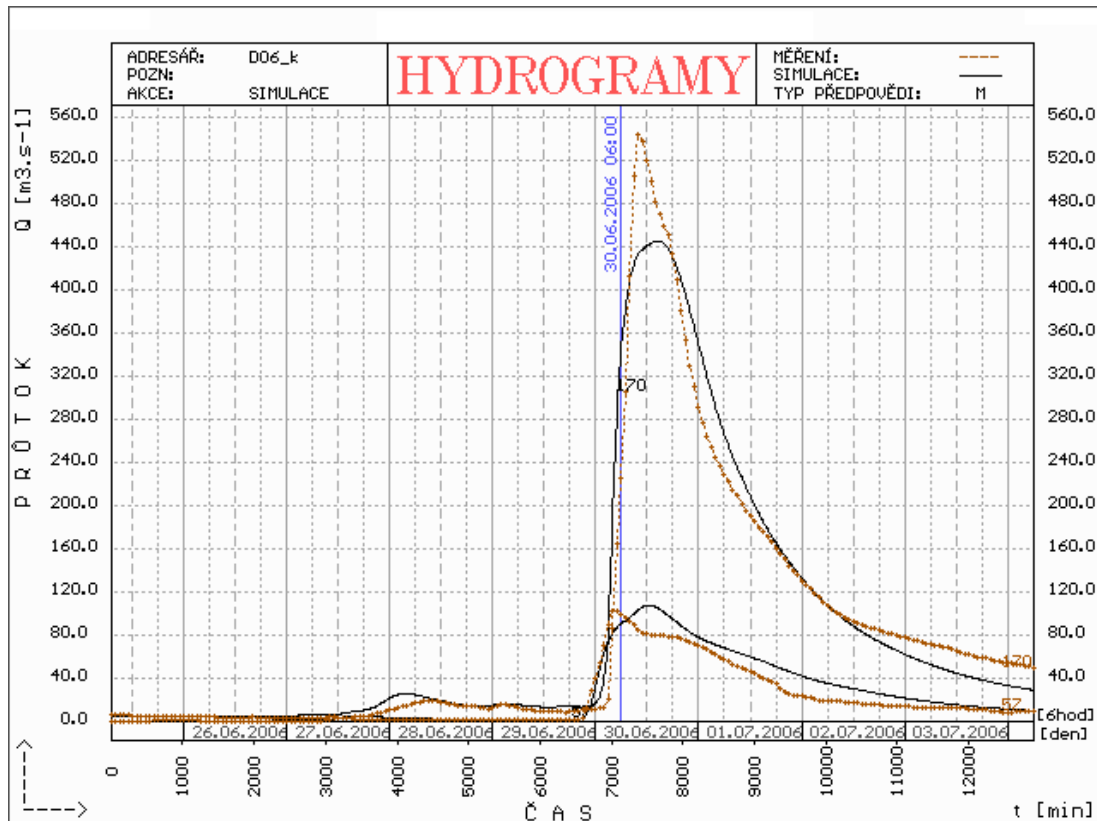


Figure 1.15. The flood event July 2006 - the simulation of discharge in Janov profile (no. 57) and Podhradí profile (no. 170) made by HYDROG model compared with measurement (brown color).

The simulation of extreme floods which occurred in August 2002, March-April 2006 and July 2006 based on reliable input data together with the results of simulations of historical floods enable us to estimate behaviour of the catchment in different periods. Further work will be now concentrated on the error of the simulation of the flood events (mainly the peak discharges), which is necessary for the evaluation of the simulation of future potential flood events based on ALADIN climate scenario. It is necessary also to analyse the past from the point of view of return time period peak discharges in important profiles.

### 1.3. References

- Březková, L., Soukalová, E. (2006): Operative hydrological forecast in winter season – floods caused by snow melting. In: Conference Proceedings XXIII. Conference of Danubian Countries on the Hydrological Forecasting and Hydrological Bases of Water management. Belgrade, p. 4. Conference Abstract, full text on enclosed CD
- Šálek, M., Březková, L. (2004): Utilization of radar-based precipitation estimate in the Czech Republic. ERAD 2004 proceedings, ERAD publication series, Vol. 2, 516-521.

## 2. Vltava River basin (Czech Republic)

The assessment of impacts of the climate change on hydrology, water quality, and management of surface water resources has been elaborated for the upper part of Vltava River basin with the modelling system consisting of two models – the precipitation-runoff and water quality model in the river network HSPF (*Bicknell et al., 2001*) and the reservoir hydrodynamics and water quality model CE-QUAL-W2 (*Cole and Wells, 2003*). The HSPF model was calibrated for hydrological simulations in the whole basin and the coupled HSPF/CE-QUAL-W2 modelling system for simulations of both hydrology and water quality in Rimov Reservoir.

### 2.1. Models and their setup

#### 2.1.1. HSPF

The HSPF model (*Bicknell et al. 2001*) is a conceptual precipitation-runoff model with a modular structure that enables simulations of transport of multiple substances from the catchment and their transformations in the river network. Simulations are accomplished in user-defined separate parts of the catchment and of the river network that have similar soil, water ecosystem, and climate conditions. The separation of the Vltava River basin was done into 67 subcatchments shown in *Figure 2.1*. Each subcatchment was composed of 5 segments that represented farmland, low-slope ( $<8^\circ$ ) areas, high-slope ( $>8^\circ$ ) areas, flood areas (maximum distance of 100 m from the channel and with slope  $<1^\circ$ ), and impervious areas. The modules comprise water balance of pervious and impervious (PWATER and IWATER), snow cover (SNOW), soil moisture (MSTL), soil erosion and transport (SEDMNT, SOLIDS), and phosphorus transport from the catchment (PHOS). The river network of each subcatchment was divided into two segments. The first, upper one represented 1<sup>st</sup> to 3<sup>rd</sup>-order (Strahler) streams and the second one streams of higher orders. Within the stream and river segments the HSPF model used modules of flow transformation (HYDR), advective transport of substances (ADCALC), transport, sedimentation, and resuspension of erosion particles (SEDTRN), nutrient transformations (NUTRX) a phytoplankton growth (PLANK). The model outputs in a format of text files are used as input files for the subsequent simulations with the reservoir model CE-QUAL-W2.

The hydrology of the Vltava River basin was calibrated in six larger sets. Their layout is shown in *Figure 2.1* and their characteristics are in *Table 2.1*. The data on precipitation, potential evaporation (PET), and temperature in a daily time step were used as model inputs for the period 1961–2004. Daily precipitation amounts were acquired from the Czech Hydrometeorological Institute (CHMI) from 49 precipitation and climatic stations. Missing values (35%) were filled in by the method of nearest neighbour combined with simple linear regression. Then precipitation for each subcatchment was calculated according to method of Thiessen polygons. Daily PET was computed by the approach of FAO Penman-Monteith equation for reference crop from air temperature, relative humidity, cloud cover, and wind velocity datasets. These datasets come from the CHMI climatic station České Budějovice (CB, 388 m a. s. l.) in the centre of studied area. Wind velocity was replaced by 12 average monthly values for 61–04 period to achieve homogeneity of calculated evapotranspiration. PET was corrected for each simulated subcatchment by a multiplicative coefficient (1.0–1.9) in the calibration procedure. The air temperature from the CB station was shifted in the HSPF model internally (module ATEMP) in the dependence on the median elevation of subcatchment (lapse rate 0.55–0.6 °C/100 m). The areas of HSPF simulation sets and the numbers of subcatchments and precipitation stations are in *Table 2.1*. The HSPF model was calibrated against daily datasets of flow with various lengths (9 to 44 years) in respect to the gradual development of the observation network of CHMI and the availability of data. The final calibration was done at the closing profiles for each HSPF

simulation set to the mean monthly observed flows during the whole period (1961-2001).

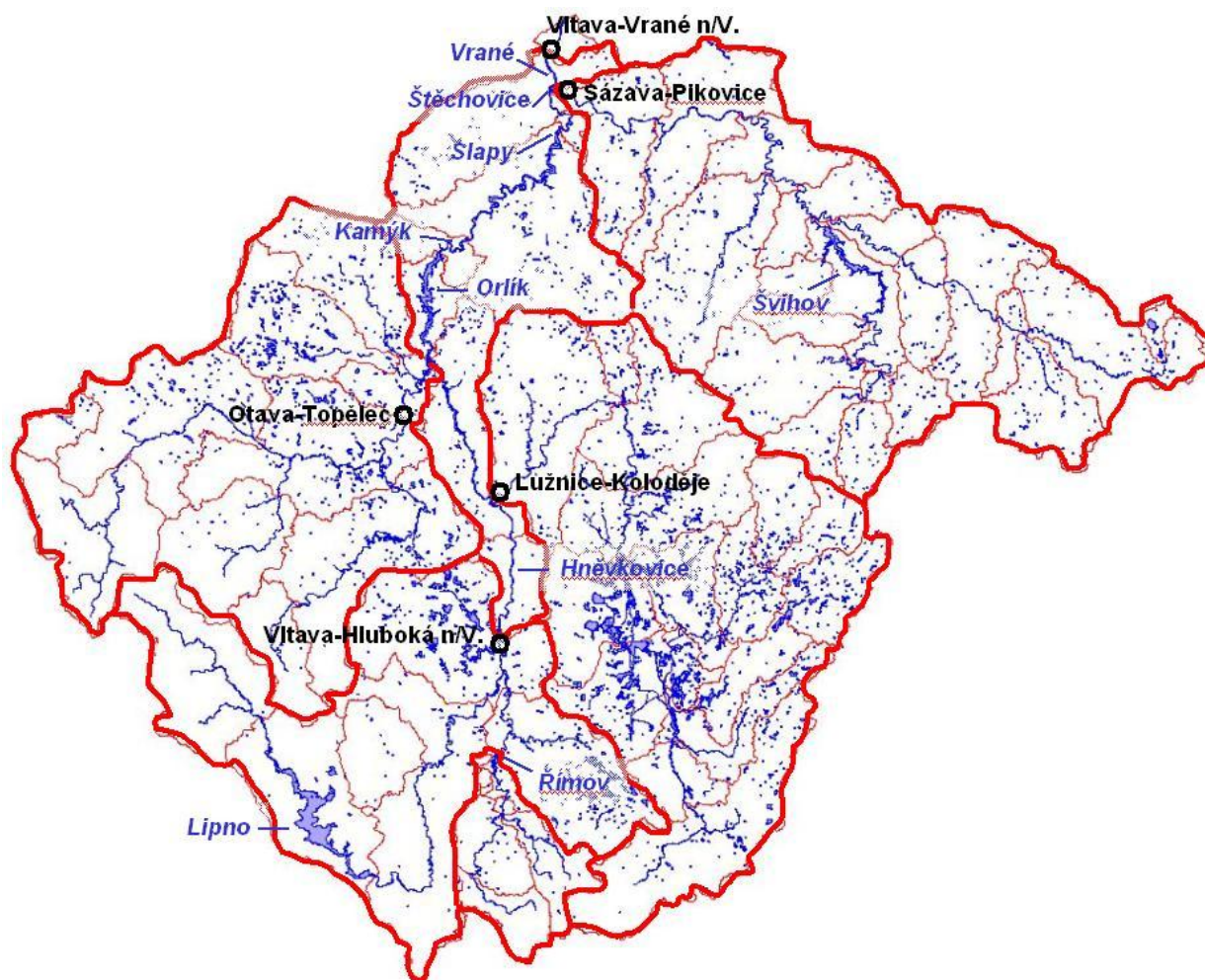


Figure 2.1 The upper Vltava River basin with major rivers and reservoirs. Circles – selected hydrology stations; thick red line – the main HSPF simulation sets; little red line – the subcatchments.

Table 2.1 Information about the HSPF simulation sets

Characteristic	Malse-Rimov (R)	Vltava-Hluboka n/V. (H)	Luznice (L)	Otava (O)	Sazava (S)	Vltava-Vrané n/V. (V)
Area, km <sup>2</sup>	489	3395	4233	3840	4349	1487
No. of subcatchments	8	6	16	10	20	7
No. of precipitation stations	11	18	11	16	11	7
No. of hydrometric calib. profiles	4	6	12	10	17	2
Links from other simulation sets	no	R	no	no	no	H, L, O, S

The coupled catchment-reservoir model was calibrated in a daily step for the catchment of Rimov Reservoir (5 subcatchments) in the period 1991–2003. Input data comprised daily precipitation amounts, air and water temperatures, potential evapotranspiration, and total phosphorus (TP) in atmospheric deposition, which represented each subcatchment. Input of P from point sources was aggregated for the subcatchment and linked directly to river segments. HSPF output time series of orthophosphate phosphorus (PO<sub>4</sub>-P), and undifferentiated (mineral and organic) particulated phosphorus (PP) was passed to CE-QUAL-W2 as inputs. Modelling system was calibrated for the period from November 1, 1998 to October 31, 2003 (five hydrological years). The hydrologic part was calibrated against daily discharges measured at 3

hydrologic profiles in the catchment. Water quality was calibrated against measured concentrations of total suspended solids (TSS), dissolved P (DP) as a representative of PO<sub>4</sub>-P, and PP in the main tributary to Rimov Reservoir (profile Malse-Poresin; 94% of total water inputs) with the weekly composite samples.

### 2.1.2. CE-QUAL-W2

The two-dimensional, laterally averaged numerical reservoir model CE-QUAL-W2 v. 3.2 (Cole and Wells, 2003) was used. The Rimov Reservoirs was approximated with a finite-difference grid that consisted of segments 300 m to 1 km in length and 0.5 to 1 m thick. Water quality simulations included the following quantities: temperature, water age, dissolved oxygen, biomass of 3 phytoplankton groups (ALG1, ALG2, ALG3), labile and refractory dissolved and particulate organic matter (LDOM, RDOM, LPOM, RPOM), orthophosphate P (PO<sub>4</sub>-P), NO<sub>3</sub>-N, and NH<sub>4</sub>-N. The model was calibrated and validated in the same periods as the HSPF model. The reservoir hydrodynamics were calibrated against vertical profiles of water temperature that were measured at the Rimov Reservoir dam in the deepest point above the original river channel. The dynamics of chemical and biological changes in the reservoir were set for measured concentrations of dissolved oxygen, dissolved phosphorus (DP), total phosphorus (TP), and chlorophyll-a (ChlA) in the surface layer at the dam. An independent validation with inputs from the HSPF model (discharge, concentration of PO<sub>4</sub>-P) was done for the period from January 1, 1991 to December 31, 2003.

### 2.1.3. Evaluation of model efficiency

The model efficiency and reliability of simulations were evaluated by selected statistical parameters: (i) mean values of observed (AVG-poz.) and simulated (AVG-sim.) values, (ii) mean of absolute error (AME), (iii) root mean square error (RMSE), (iv) mean relative error (RE), and (v) Nash-Sutcliffe coefficient of model efficiency (NS; Nash and Sutcliffe 1970) that gives values close to 1 for good agreement between observed and simulated values and values <0 for simulations that have lower prediction force than the mean of observed values.

## 2.2. Model calibration

### 2.2.1. Hydrology of the Vltava River basin

The HSPF model calibration results for hydrology in the main catchments of the Vltava River basin on the mean monthly flow basis are given in *Table 2.2* and *Figure 2.2*. The agreement between the simulated and observed values was acceptable in all profiles. The relative error ranged from 0.03 to 0.21 and the Nash-Sutcliffe coefficient from 0.51 to 0.77.

*Table 2.2. Results of calibration for closing profiles of HSPF simulation sets 1961–2004 for mean monthly flow values (n = 535)*

	Malse-Rimov (R)	Vltava-Hluboka n/V. (H)	Luznice (L)	Otava (O)	Sazava (S)	Vltava-Vrane n/V. (V)
AME	1.29	7.7	7.8	6.3	9.1	25.9
RMSE	0.48	0.38	0.48	0.33	0.61	0.33
RE	0.09	0.03	0.21	0.08	0.19	0.06
NS	0.65	0.62	0.69	0.78	0.51	0.77
AVG-sim, m <sup>3</sup> s <sup>-1</sup>	4.27	29.0	22.9	27.9	25.1	117.6
AVG-poz, m <sup>3</sup> s <sup>-1</sup>	4.24	29.0	23.2	27.5	24.8	117.0

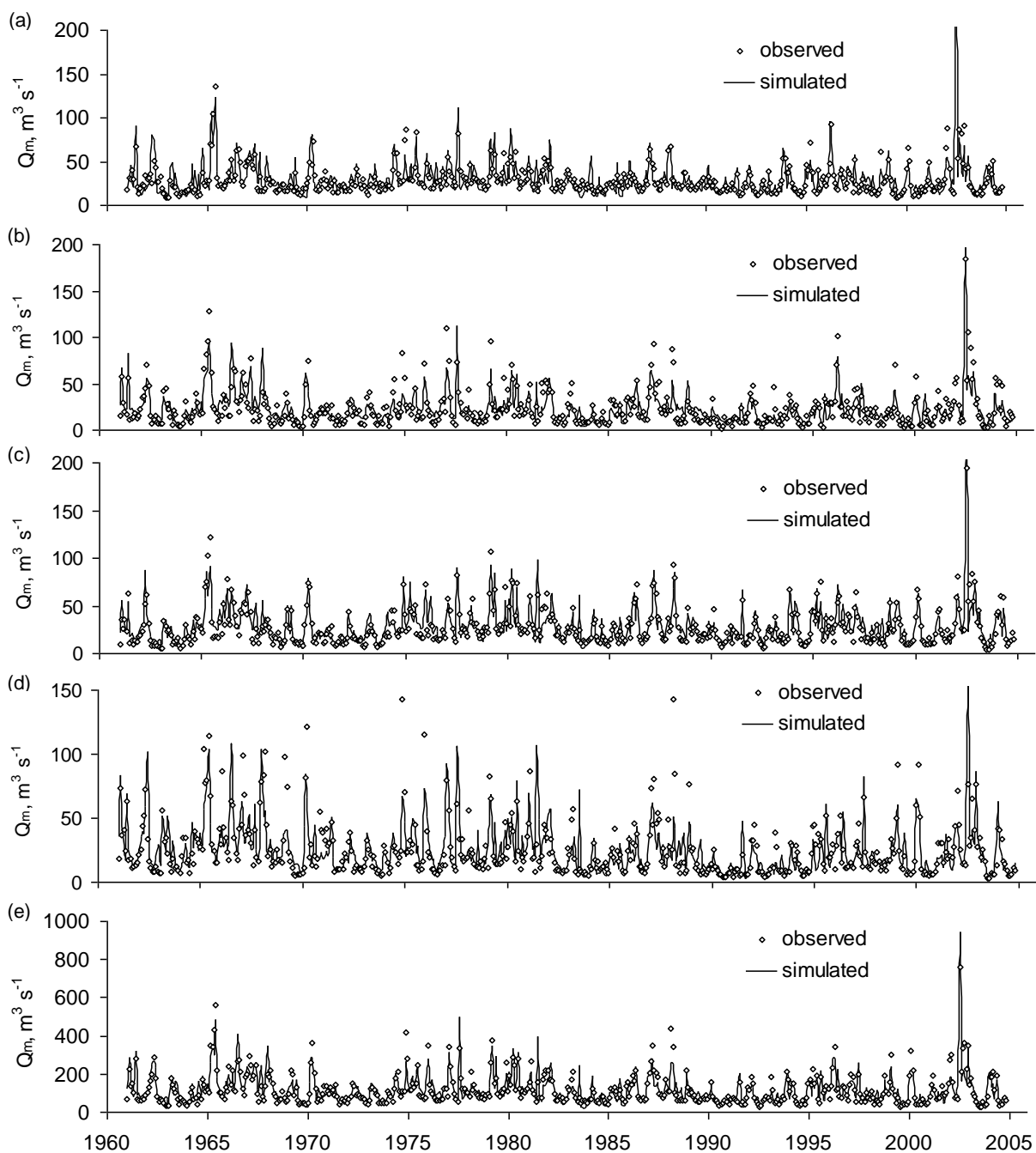


Figure 2.2. Comparison of HSPF-simulated and observed mean monthly flows in the main catchments of the Vltava River basin (a) Vltava-Hluboka n/V., (b) Luznice, (c) Otava, (d) Sazava, and (e) Vltava-Vrane n/V.

### 2.2.2. Water quality in Rimov Reservoir

The results of hydrological calibration of the HSPF model for the inflow into the reservoir at a daily time step are given in *Table 2.3* and *Figure 2.3*. The model realistically described the seasonal pattern of base flow changes both in periods of higher flow during spring snow melt and during periods of decreasing flow in late summer and autumn. Runoff events following heavy rains were simulated usually also well, including the catastrophic flood in August 2002. A lower precision of the validation run was probably caused mainly by inhomogeneities in the input data, especially precipitation and discharge measurements and/or evapotranspiration.

Table 2.3. Comparison of simulated and observed daily flow ( $Q_d$ ) in the main inflow of Rimov Reservoir during the calibration and validation periods

Parameter	cal. 99-03	val. 91-98
AME	1.48	1.35
RMSE	4.23	2.59
RE	0.09	-0.07
NS	0.85	0.71
AVG-sim.	4.26	3.47
AVG-poz.	4.30	4.00

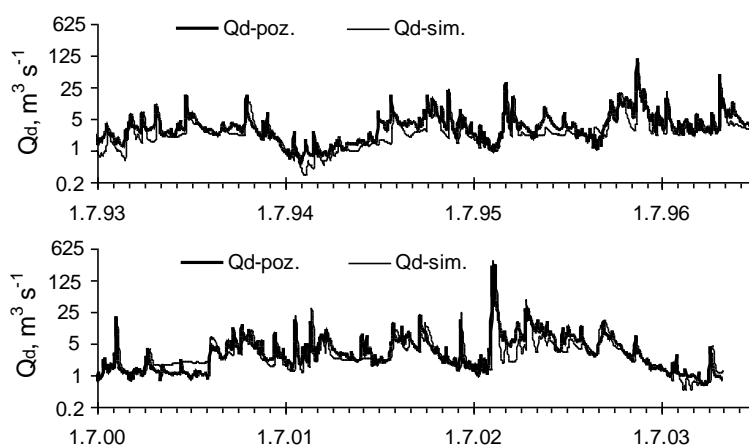


Figure 3.3. Observed ( $Q_{d-poz.}$ ) and simulated ( $Q_{d-sim.}$ ) daily discharge in the profile Malse-Poresin during selected parts of calibration period (bottom) and validation period (top).

The calibration results for the HSPF simulations of phosphorus forms in the main inflow of Rimov Reservoir are in Table 2.4 and Figure 2.4. The main source of DP in the Rimov Reservoir catchment were point sources. Therefore, the seasonal pattern of DP concentration in the inflow was largely influenced by the dilution of almost constant input of P from municipal wastewater. The HSPF model correctly simulated the high summer concentrations except for the August-to-October period 2003 when the simulated flow was underestimated by ca  $0.5 \text{ m}^3 \text{ s}^{-1}$  (i.e. more than 50%). The simulation of PP was largely connected with the transport of erosion particles from the catchment. The model reproduced only large erosion events. The seasonal fluctuation of the background PP concentration (in the range from 5 to  $20 \mu\text{g l}^{-1}$ ) was captured by the model only partially (Figure 2.4). A plausible explanation for this difference might be the negligence of organic PP in the model or an imprecise adjustment of model parameters for particle sedimentation and remobilisation in the rive network.

Table 2.4. Comparison of HSPF-simulated and observed concentrations of TSS, DP, and PP in the profile Malse-Poresin in the calibration ( $n=324$ ) and validation ( $n=139$ ) periods

Parameter	TSS, $\text{mg l}^{-1}$		DP, $\mu\text{g l}^{-1}$		PP, $\mu\text{g l}^{-1}$	
	cal. 99-03	val. 91-98	cal. 99-03	val. 91-98	kal. 99-03	val. 91-98
AME	12.4	3.3	20.6	19.8	28.9	19.8
RMSE	37.5	5.65	29.7	29.2	79.9	29.3
RE	0.97	0.55	0.10	0.06	0.23	0.58
NS	0.17	-0.17	0.24	0.75	0.16	-0.30
AVG-sim.	12.2	3.9	53.3	78.7	33.0	35.9
AVG-poz.	15.3	4.7	53.6	78.0	49.1	31.4

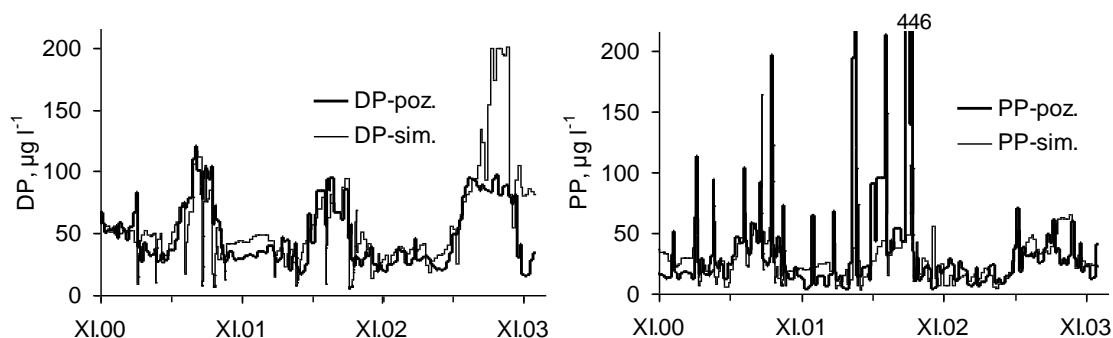
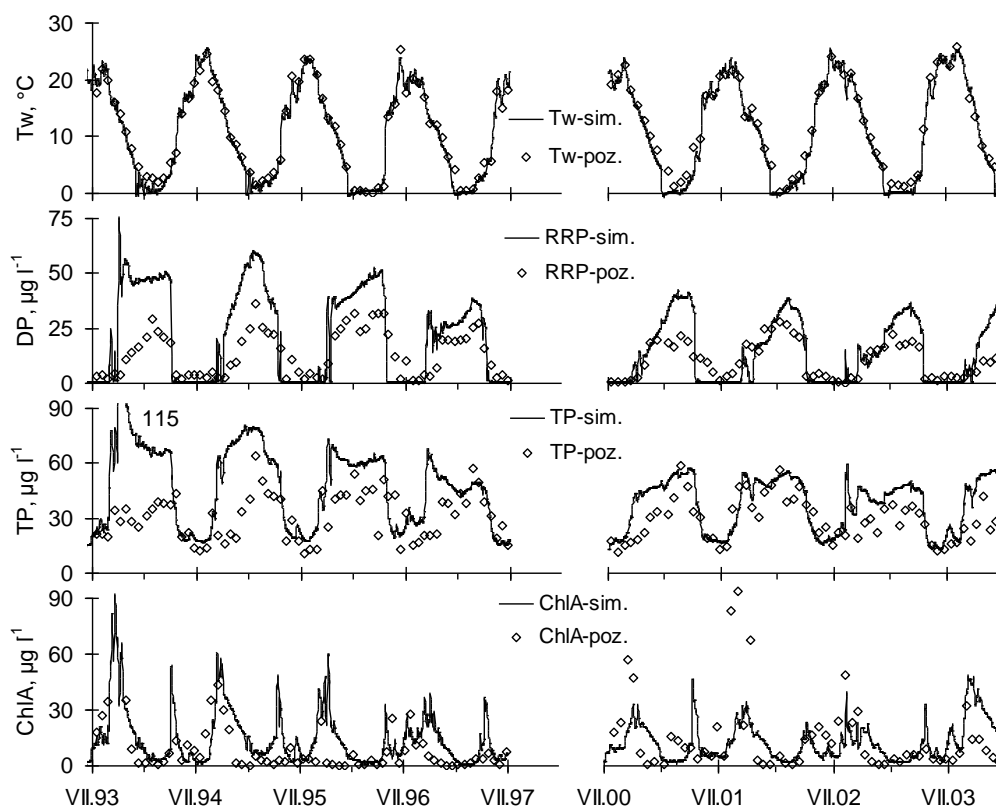


Figure 2.4. Observed and simulated concentrations of DP and PP in the main inflow into Rimov Reservoir (profile Malse-Poresin)

The comparison of observed and simulated water temperatures and concentrations of DP, TP, and ChlA in Rimov Reservoir with the model system HSPF–CE–QUAL–W2 is given in *Figure 2.5*. The simulated reservoir hydrodynamic variables and temperature stratification were in a good agreement with the measured values in all model runs ( $NS > 0.9$ ). The simulated seasonal patterns of phosphorus concentrations fitted together with the observations reasonably well during the vegetation period of year when phytoplankton was able to deplete  $PO_4\text{-P}$  in the epilimnion to very low concentrations. However, the model tended to overestimate phosphorus concentrations during the cool period of year. The largest differences occurred in the beginning of the 1990s when the P load into the reservoir was approximately twofold in comparison with the later period. The concentrations of chlorophyll-a were reproduced during both the calibration and validation periods with a low precision. This is a rather common feature of most ecological models of the aquatic ecosystem that results from the poor mathematical description of natural variability of carbon, phosphorus, and chlorophyll-a concentrations in phytoplankton cells and the necessary simplification of food web structures. The main features of the seasonal patterns of phytoplankton, i.e. the spring onset of its development and the growth response after summer inputs of P during storm inflows, were captured well by the model.



*Figure 2.5. Comparison of observed (poz.) and simulated (sim.) values of water temperature ( $T_w$ ) and concentrations of DP, TP, and ChlA in Rimov Reservoir for selected periods of calibration (2000–2003) or validation (1993–1997) of the model system HSPF–CE–QUAL–W2*

### 2.3. References

- Bicknell, B.R., Imhoff, J.C., Kittle Jr., J.L., Jobes, T.H., Donigan Jr., A.S. (2001): Hydrological Simulation Program–Fortran (HSPF). User's Manual for Release 12. U.S. EPA National Exposure Research Laboratory, Athens, GA, in cooperation with U.S. Geological Survey, Water Resources Division, Reston, VA.
- Cole, T. M., Wells, S. C. (2003): CE-QUAL-W2: A Two-Dimensional, Laterally Averaged, Hydrodynamic and Water Quality Model, Version 3.2. User Manual. Instruction Report EL-03-1. U. S. Army Corps of Engineers, Washington, DC.
- Nash, J.E., Sutcliffe J.V. (1970): River forecasting through conceptual models: Part I, A discussion of principles. *J. Hydrol.* 10, 282–290, 1970.

### 3. Hron river basin (Slovakia)

#### 3.1. Short description of the hron river basin

##### *Topography*

The Hron River is a left-side tributary of the Danube River, its basin is located in Central Slovakia. The catchment is feather-shaped, located along the long main river with numerous shorter tributaries. It covers an area of 5465 km<sup>2</sup>, its upper and middle parts are situated in the area of Inner Carpathian Mountains, while the lower part of the basin belongs to the Danubian Lowlands. The location of the catchment within the territory of Slovakia is shown in *Figure 3.1*.

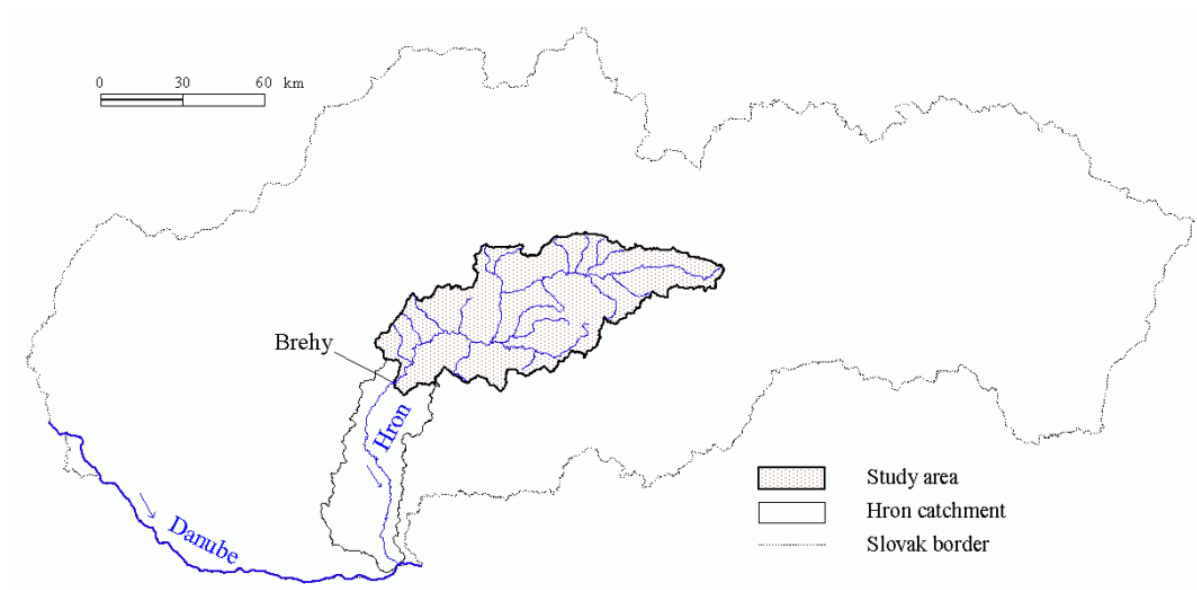


*Figure 3.1. Location of the Hron River basin in Slovakia*

With regards to the availability of hydro-meteorological data and also according to the character of the hydrologic processes in the catchment only upper regions are suitable for conceptual water balance modeling with a monthly time step. The alluvial part of the river has not sufficient data suitable for modeling (short series and less a dense network), but due to its lowland character and very low specific discharge (mostly less than 1.5 l/skm<sup>2</sup>), modeling approaches have to be applied, which better account for the physically based description of processes in the unsaturated zone than the WATBAL model and other conceptual monthly water balance models.

The lowest reliable discharge gauging station on the main river is at Brehy. This station was selected as the closing cross section for the CECILIA project (the term “Hron River basin” refers mainly to the Hron catchment to Brehy hereafter). This subcatchment has an area of 3 821 km<sup>2</sup> (8% of the Slovak territory). Its relief is represented by digital elevation model in *Figure 3.2*. Elevation ranges from 195 m a.s.l. at the catchment outlet to 2 043 m a.s.l. on the peak of Ďumbier in Nízke Tatry Mountains on the north.

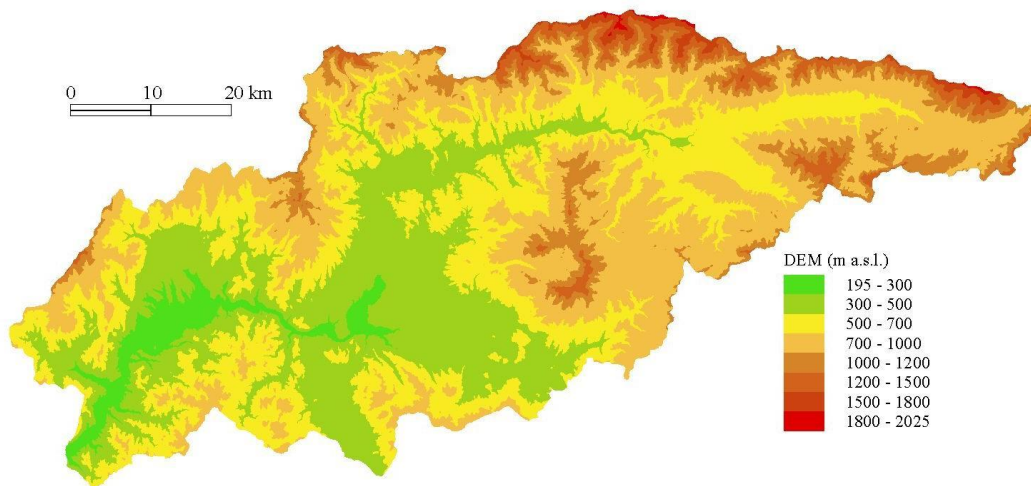


Figure 3.2. Digital elevation model (DEM) of the Hron River basin (50x50 m resolution)

### Soils and landuse

The soil texture map of the study region, which is shown in *Figure 3.3*, was constructed based on data from 2417 soil test pits within the basin. The Thiessen polygon method was used for spatial interpolation. The soil classification in *Figure 3.7* follows the USDA structure, which has 12 categories, eleven of these can be found in the Hron River basin. Silt, sandy loam and silt loam soil types prevail.

The landuse map, which is shown in *Figure 3.4*, is based on Landsat images from the year 2000 with the resolution 30 x 30 m. Images were rectified according to topographic, vegetation and silvicultural maps, which were available in the scale of 1:10 000. Fifteen landuse categories occur in the region. Fifty six percent of the area is covered by forests, 26% by arable land, 14% by meadows, pastures and shrubs and 4% by urban areas.

### Climate

The climatic conditions of the Hron River basin correspond to the European-continental climatic region of the mild zone, with oceanic air masses transforming into continental ones. The annual precipitation in the basin varies from 570 to 700 mm/year in the lowlands to about 700-1400 mm/year in the valleys and upper mountainous areas. The overall average is approximately 800 mm/year. Evaporation amounts to approximately 300 to 600 mm/year.

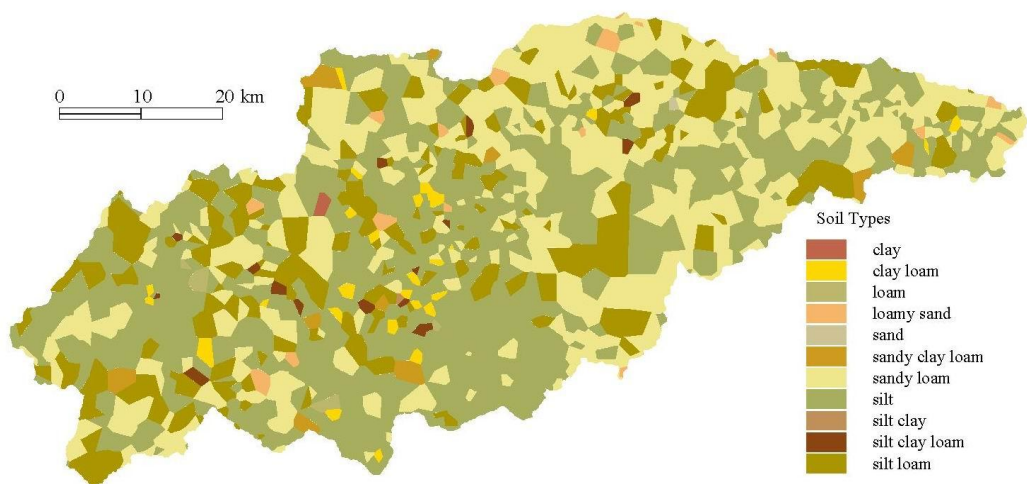


Figure 3.3. Map of the soil types of the Hron River catchment

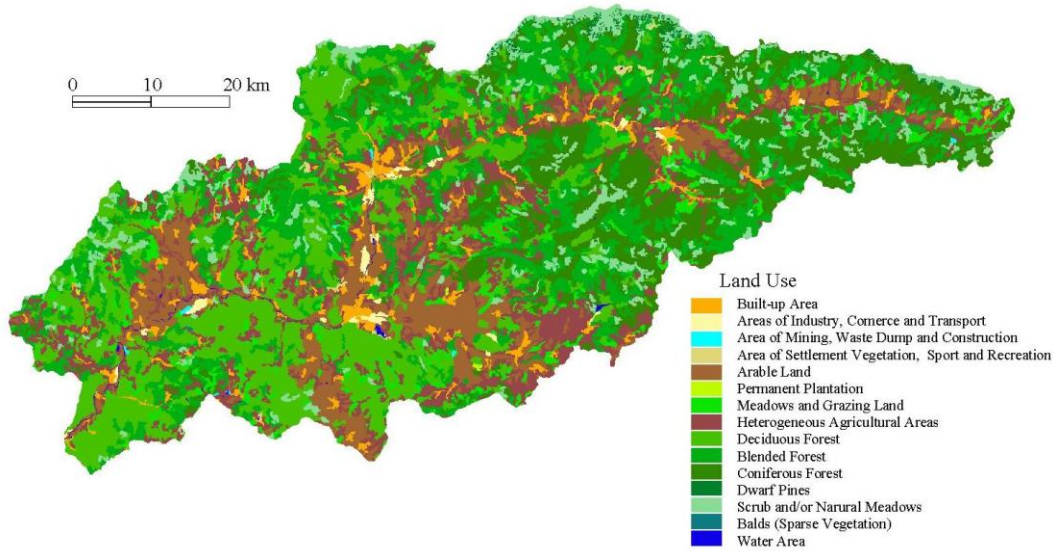


Figure 3.4. Landuse of the study region based on Landsat images from 2000

### **Meteorological and hydrologic data**

The monthly water balance model used requires time series of average monthly data of precipitation [mm], air temperature [ $^{\circ}\text{C}$ ] and runoff [ $\text{m}^3 \cdot \text{s}^{-1}$ ] as a minimum. These can be extended by data required for potential evapotranspiration estimation.

Daily precipitation data for the study area are measured in 44 rain gauge stations; daily temperature data are available from 12 climatic stations (Figure 3.5). Long term monthly potential evapotranspiration data calculated by Tomlain and Damborská (1999) according to the Budyko method is available at the climatic stations.

Available and good quality data determined the selection of the time period and catchments for the study. The necessary condition of data from the period 1970 to 2000 is met in all selected stations. Moreover it was decided to include only stations, where data from 1961 were also available for model verification. More detailed description of the data is in the part “Calibration of the hydrological model”.

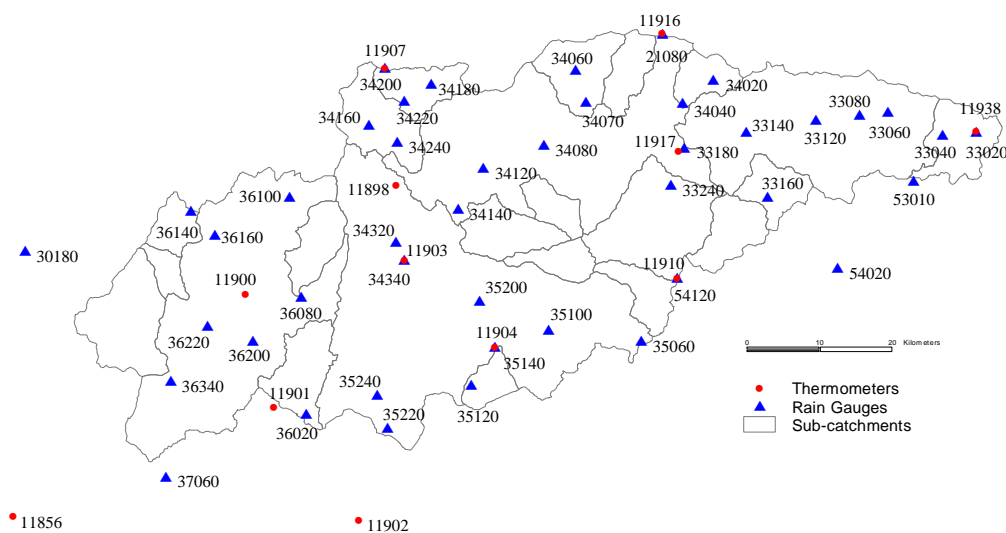


Figure 3.5. Location of the rain gauges and climatic stations with reliable data in region

### 3.2. Description of the KVHK hydrological balance model

For estimating the changes in the seasonal runoff distribution, the conceptual hydrological balance model KVHK developed at the Slovak University of Technology will be used. This model is a refinement of the Watbal model which was chosen as a reference model in the CECILIA project. The KVHK model simplifies the river basin into 2 nonlinear reservoirs, and it simulates runoff from impermeable areas in the basin, snowmelt and water accumulation in the basin, evapotranspiration, surface and subsurface runoff and baseflow. The inputs required for the modelling water balance in a monthly time step are: the mean monthly precipitation for the basin, the mean monthly discharges in the outlet of the basin and the mean monthly potential evapotranspiration (*PET*). For calculating the potential evapotranspiration, various methods can be used (the Tomlain, Thornthwaite, Ivanov and FAO methods) and additional climate data (the mean monthly air temperature values, the mean monthly hours of sunshine duration, the mean monthly values of the relative air humidity, the mean monthly values of wind speed, the monthly values of cloudiness and number of days with snow cover in a month) are required.

The basic mass balance equation in the model is written as:

$$S_i - S_{i-1} = (P_i(1 - drc)) - R_{s_i} - R_{ss_i} - Ev_i - R_b \quad (3.1)$$

where:

- $S_i, S_{i-1}$  - current water storage in the basin in months  $i$  and  $i-1$  [mm],
- $i$  - time step [month],
- $P_i$  - basin's average precipitation in the month  $i$  [mm],
- $drc$  - direct runoff coefficient ( $0 \leq drc \leq 1$ ) [-],
- $R_{s_i}$  - surface runoff in the month  $i$  [mm],
- $R_{ss_i}$  - subsurface runoff in the month  $i$  [mm],
- $Ev_i$  - basin's average actual evapotranspiration in the month  $i$  [mm],
- $R_b$  - baseflow [mm].

The scheme of the model is illustrated in *Figure 3.6*.

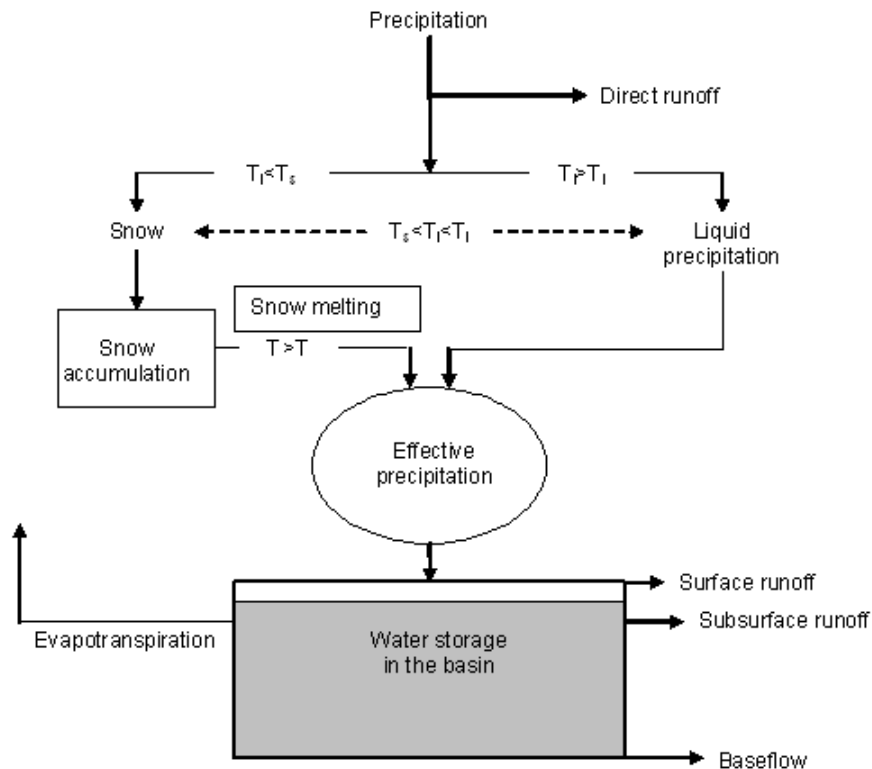


Figure 3.6. Scheme of the hydrological balance model.

At the beginning of simulation a part of the precipitation fallen down to impermeable or the water surface is extracted as a direct runoff. The rest of the precipitation goes to the first snowmelt and snow accumulation nonlinear reservoir, which enables distinction between solid and liquid precipitation on the basis of the threshold temperatures. In this reservoir, the effective precipitation which further participates on the runoff formation is calculated as:

$$P_{eff_i} = mc_i (A_{i-1} + P_i) \quad (3.2)$$

Where:  $mc_i = 0$  if  $T_i \leq T_s$

$mc_i = 1$  if  $T_i \geq T_l$

$$mc_i = \left[ \frac{(T_i - T_s)}{(T_l - T_s)} \right]^{P_{effPar}} \quad \text{if } T_s < T_i < T_l \quad (3)$$

$P_{eff_i}$  - effective precipitation for the basin in the month  $i$  [mm],

$P_i$  - basin's average measured precipitation in the month  $i$  [mm],

$A_{i-1}$  - snow accumulation in the month  $i-1$  [mm],

$mc_i$  - snow melting factor in the month  $i$  [-],

$T_i$  - mean air temperature in the month  $i$  [°C],

$P_{effPar}$  - parameter for calculating basin's average effective precipitation [-],

$T_s$  - threshold air temperature for snow accumulation [°C],

$T_l$  - threshold air temperature for snow melting [°C].

If the current air temperature in the month  $i$  is higher than the threshold temperature  $T_l$ , all precipitation is considered to be liquid and it will participate on runoff formation in this month. If the current air temperature is lower then the threshold temperature  $T_s$ , all precipitation is accumulated in the snow cover. In the case if the current air temperature is in between  $T_s$  and  $T_l$  ( $T_s < T_i < T_l$ ), a part of liquid and a part of accumulated precipitation is calculated according to the snow melting factor  $mc$ . Relationships between the snow melting factor and the mean monthly air temperature are shown in *Figure 3.7*, these are controlled by the model parameter  $P_{effPar}$ .

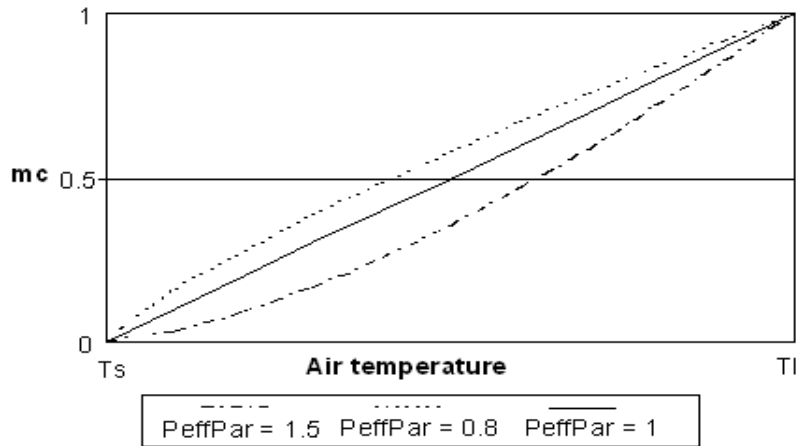


*Figure 3.7. Relation between the snow melting factor, the mean monthly air temperature and the  $P_{effPar}$  parameter.*

Snow accumulation is calculated by the equation:

$$A_i = (1 - mc_i)(A_{i-1} + P_i) \quad (3.3)$$

where:  $A_i$  and  $A_{i-1}$  is snow accumulation in months  $i$  and  $i-1$  [mm].

Surface runoff  $R_s$  is calculated as a function of the ratio between the current and maximum water storage in the second nonlinear (water accumulation) reservoir, parameter  $\varepsilon$  and a difference between effective precipitation and baseflow  $R_b$ . The baseflow  $R_b$  is a model parameter. If the effective precipitation in the month  $i$  is lower than the baseflow value, surface runoff is equal zero. Otherwise, the surface runoff is expressed as:

$$R_{s_i} = \left( \frac{S_i}{S_{\max}} \right)^\varepsilon (P_{\text{eff}_i} - R_b) \quad (3.4)$$

where:

- $S_{\max}$  - maximum water storage in the second nonlinear reservoir [mm],
- $S_i$  - current water storage in the second nonlinear reservoir in the month  $i$  [mm],
- $P_{\text{eff}_i}$  - effective precipitation in the month  $i$  [mm],
- $R_b$  - baseflow [mm],
- $\varepsilon$  - a model parameter [-].

Subsurface runoff is a function of the ratio between current and maximum water storage in the second water accumulation reservoir, and parameters  $\alpha$  and  $\gamma$ :

$$R_{ss_i} = \alpha \left( \frac{S_i}{S_{\max}} \right)^\gamma \quad (3.5)$$

Actual monthly evapotranspiration for the basin is calculated as a function of monthly potential evapotranspiration for the basin and the ratio between current and maximum water storage in the second water accumulation reservoir. Actual monthly evapotranspiration is than expressed in the form:

$$E_{v_i} = E_{0_i} \left[ 1 - \left( 1 - \left( \frac{S_i}{S_{\max}} \right) \right) \right]^{\text{ActEpar}} \quad (3.6)$$

Where:  $E_{0_i}$  is the potential evapotranspiration in the month  $i$  and  $\text{ActEpar}$  is a model parameter.

The total runoff  $R_t$  is calculated as the sum of the four runoff components  $R_s$ ,  $R_{ss}$ ,  $R_b$  and  $R_d$ , where  $R_d$  is direct runoff.

In the calibration procedure of the hydrological balance model, 11 model parameters are optimized ( $S_{\max}$ ,  $\alpha$ ,  $\gamma$ ,  $\varepsilon$ ,  $P_{\text{effPar}}$ ,  $T_s$ ,  $T_l$ ,  $R_b$ ,  $\text{ActEpar}$ ,  $drc$  and  $Z_{\text{initial}}$ ). The parameter  $Z_{\text{initial}}$  is an initial value of the ratio between  $S_i$  and  $S_{\max}$ . In the model a genetic algorithm (GA) is built in to calibrate the model parameters for the at site data, and several criteria (or their combinations) are used as an objective function. Basic optimization criteria are the Nash-Sutcliffe criterion, the sum of squared differences between measured and simulated values, the sum of squared differences between logarithms of measured and simulated values and the Nash-Sutcliffe criterion for the long-term mean monthly values.

### 3.3. Calibration of the hydrological model

The KVHK hydrological balance model was calibrated and validated in selected sub-basins of the Hron river basin on data from the period of 1971-2000 (calibration period) and 1961-1970 (validation period). Three sub-basins have outlets directly at the Hron River (Brezno, Banská Bystrica and Brehy), others represent the Hron river tributaries. Most of the selected sub-basins can be consider as uninfluenced, only 2 sub-basins of the Slatina tributary are influenced by water reservoirs on the Slatina River (Slatina – Môt'ová and Slatina – Zvolen). For 2 sub-basins (Slatina - Hriňová and Slatina - Zvolen) discharge data only for the calibration period were available. The list of selected sub-basins is shown in *Table 3.1*.

Table 3.1. List of selected sub-basins in the Hron river basin

Basin ID	River	Gauging station	Basin area [km <sup>2</sup> ]
7015	Hron	Brezno	508.82
7160	Hron	Banská Bystrica	1766.48
7290	Hron	Brehy	3821.38
7070	Vajskovský potok	Dolná lehota	53.02
7280	Kľak	Žarnovica	131.95
7045	Čierny Hron	Hronec	239.41
7180	Slatina	Hriňová	51.99
7205	Slatina	Môľová	411.02
7230	Slatina	Zvolen	790.16

As input data the mean monthly precipitation for the sub-basins, the mean monthly discharges in the sub-basin outlets and the mean monthly potential evapotranspiration (*PET*) in the sub-basins were used. For calculating the potential evapotranspiration, the Tomlain method based on the Budyko methodology has been chosen and additional climate data for this purpose were collected: the mean monthly air temperature values, the mean monthly values of the relative air humidity, the monthly values of cloudiness and number of days with snow cover in a month.

Sub-basin's average values of monthly precipitation totals and mean monthly air temperature were estimated by the method of Thiessen polygons.

Precipitation and climate stations with precipitation and climate data from the period of 1961-2000 are listed in *Tables 3.2* and *3.3*. The map of whole region (the Hron-Brehy sub-basin) with sufficient precipitation and climate stations with data from 1961-2000 and gauging stations is shown in *Figure 3.8*.



Figure 3.8. Precipitation, climate and gauge stations with data from 1961-2000

Table 3.2. List of precipitation stations and periods with sufficient precipitation data

<b>ID</b>	<b>Precipitation station</b>	<b>Altitude (m a. s. l.)</b>	<b>Period with available data</b>
34320	Badín	372	1961 – 2006
33140	Beňuš	550	1961 – 2006
33180	Brezno	490	1961 – 2006
34080	Brusno	415	1961 – 2006
33240	Čierny Balog – Krám	522	1961 – 2006
21080	Chopok	2008	1961 – 2006
35100	Detva	443	1961 – 2006
35060	Detvianska Huta	825	1961 – 2006
35240	Dobrá Niva	366	1961 – 2006
36220	Hliník nad Hronom	237	1961 – 2006
34070	Jasenie	537	1961 – 2006
54120	Lom nad Rimavicou	1018	1961 – 2006
34180	Motyčky	650	1961 – 2006
34140	Môlča	459	1961 – 2006
34040	Mýto pod Ďumbierom	610	1961 – 2006
33160	Pohronská Polhora	637	1961 – 2006
33120	Polomka	607	1961 – 2006
37060	Pukanec	348	1961 – 2006
36200	Sklené Teplice	368	1961 – 2006
34120	Slovenská Ľupča	370	1961 – 2006
34220	Staré Hory	475	1961 – 2006
33020	Telgárt	901	1961 – 2006
36080	Trnavá Hora – Jalná	268	1961 – 2006
30180	Veľké Uherce	210	1961 – 2006
35140	Vígľač Pstruša	368	1961 – 2006
35120	Vígľašská Huta – Kalinka	527	1961 – 2006
36340	Žarnovica	218	1961 – 2006

Table 3.3. List of climate stations and periods with sufficient climate data

<b>ID</b>	<b>Climate station</b>	<b>Altitude (m a. s. l.)</b>	<b>Period with available data</b>
11901	Banská Štiavnica	575	1961 – 2006
11902	Bzovík	355	1961 - 2006
11916	Chopok	2008	1955 - 2006
11910	Lom nad Rimavicou	1018	1962 - 2006
11903	Sliach	313	1951 - 2006
11938	Telgárt	901	1951 - 2006
11904	Vígľaš – Pstruša	368	1961 - 2006

### 3.4. Results of hydrological model calibration and validation

In the following part examples of the calibration and validation results for the Hron – Banská Bystrica and Hron – Brehy sub-basins are illustrated. Time series of simulated and observed mean monthly discharges for the calibration and validation period are compared in *Figures 3.9-3.10* and *Figures 3.15-3.16*, comparison of the long-term mean monthly discharges is shown in *Figures 3.11-3.12* and *Figures 3.17-3.18*. Relationships between observed and simulated mean monthly discharges are compared in *Figures 3.13 - 3.14* and *Figures 3.19 - 3.20*. Parameters of the hydrological model for these sub-basins are shown in *Tables 3.5* and *3.6*.

For all sub-basins, the model performance was optimized by the Nash-Sutcliffe optimization criterion. In *Table 3.4* values of Nash - Sutcliffe criteria are summarized for the calibration and validation periods in all selected sub-basins. According to this criterion and also to the graphical comparisons of simulated and observed mean monthly and long-term mean monthly discharges, a good performance of the model almost in all sub-basins can be confirmed. As it was expected, the best results have been achieved for larger sub-basins with outlets at the Hron River, worse results were reached for smaller sub-basins at the Hron River tributaries. Almost in all sub-basins a slight underestimation of simulated long-term mean monthly discharges in the spring season (March and April) can be seen. In 2 influenced sub-basins (Slatina – Môťová and Slatina – Zvolen) an impact of water reservoirs is evident, especially in comparison of the long-term mean monthly discharges at the sub-basins outlets. Observed long-term mean monthly discharges are systematically lower here than simulated values nearly in all months and the difference is approximately equal to monthly water withdrawals from reservoirs.

From the comparison of results for larger and smaller basins it is evident that the hydrological model in monthly time step is more suitable for modelling runoff in larger basins. Smaller basins as Vajskovský potok - Dolná Lehota and Slatina – Hriňová (with areas approximately of 50 km<sup>2</sup>), and the Kľak - Žarnovica basin (with the area of 130 km<sup>2</sup>) because of quicker processes of runoff formation and water balance dynamics are not very suitable for modelling runoff in monthly time step. For the climate change impact study in the CECILIA project only larger basins with outlets at Brezno, Banská Bystrica, Brehy and Hronec with areas larger than 200 km<sup>2</sup> can be suggested. Influenced basins on the Slatina river can be recommended only if the effect of water reservoirs will be considered in the runoff modeling.

*Table 3.4. Values of the Nash –Sutcliffe criterion for the calibration and validation period in all sub-basins*

Sub-basin	Nash – Sutcliffe	
	Calibration 1971-2000	Validation 1961-1970
7015 Hron – Brezno	0.791	0.813
7160 Hron – Banská Bystrica	0.826	0.819
7290 Hron – Brehy	0.819	0.852
7070 Vajskovský potok – Dolná Lehota	0.665	0.653
7280 Kľak – Žarnovica	0.686	0.593
7045 Hronec – Čierny Hron	0.729	0.758
7180 Slatina – Hriňová	0.685	-
7205 Slatina – Môťová	0.717	0.764
7230 Slatina – Zvolen	0.740	-

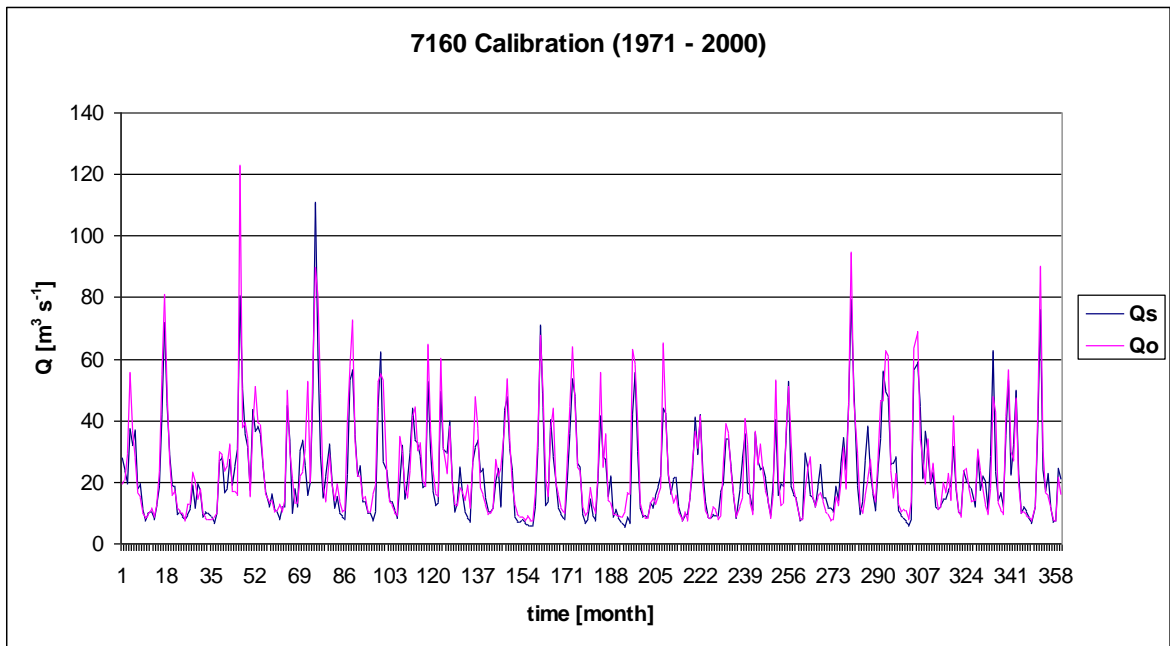


Figure 3.9. Comparison of simulated ( $Q_s$ ) and observed ( $Q_o$ ) mean monthly discharges at the Hron – Banská Bystrica gauging station for the calibration period 1971-2000

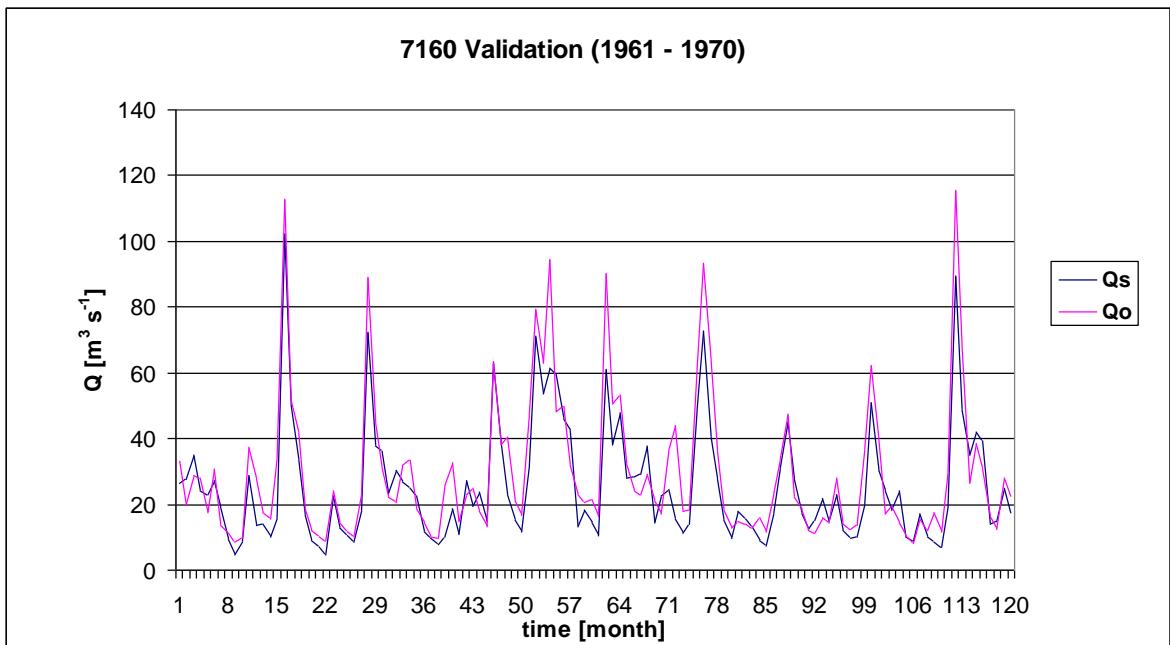


Figure 3.10. Comparison of simulated ( $Q_s$ ) and observed ( $Q_o$ ) mean monthly discharges at the Hron – Banská Bystrica gauging station for the validation period 1961-1970

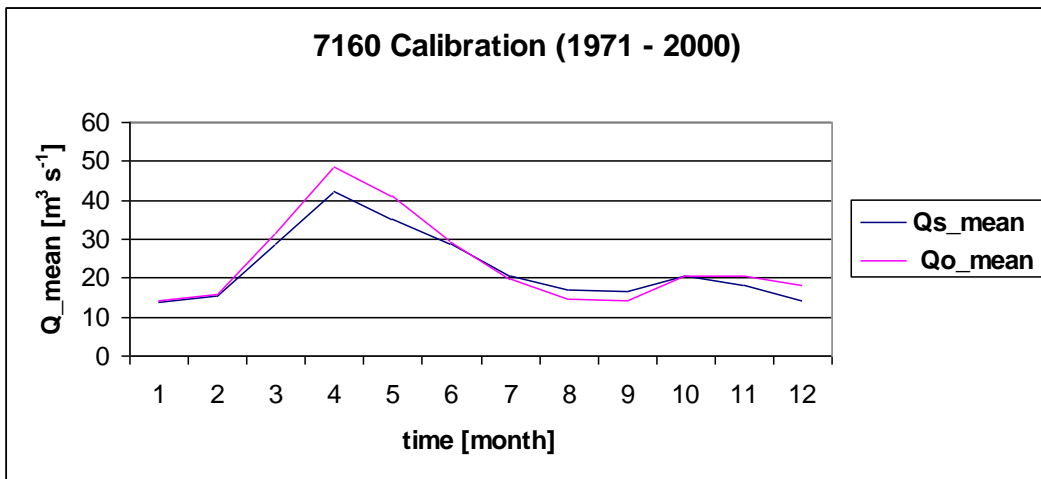


Figure 3.11. Comparison of simulated ( $Q_s\_mean$ ) and observed ( $Q_o\_mean$ ) long-term mean monthly discharges at the Hron – Banská Bystrica gauging station for the calibration period 1971-2000

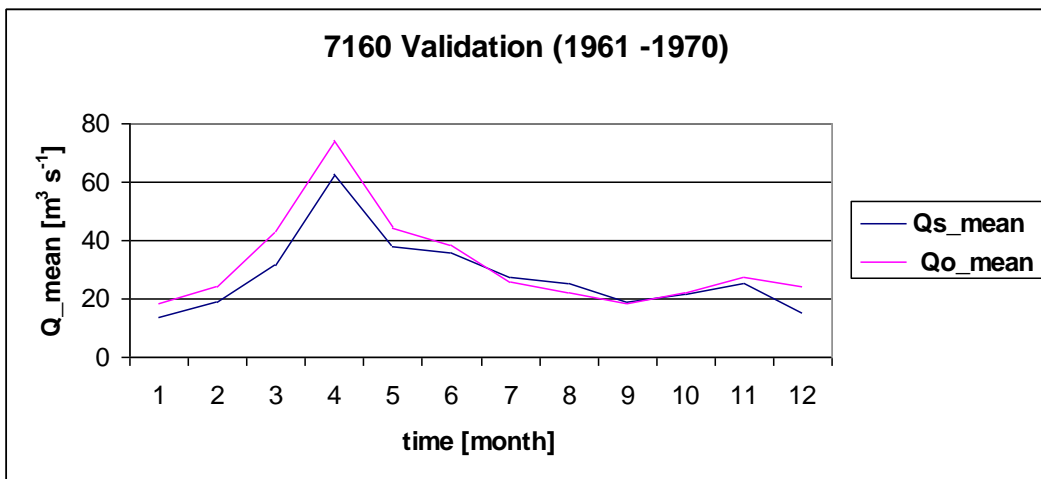


Figure 3.12. Comparison of simulated ( $Q_s\_mean$ ) and observed ( $Q_o\_mean$ ) long-term mean monthly discharges at the Hron – Banská Bystrica gauging station for the validation period 1961-1970

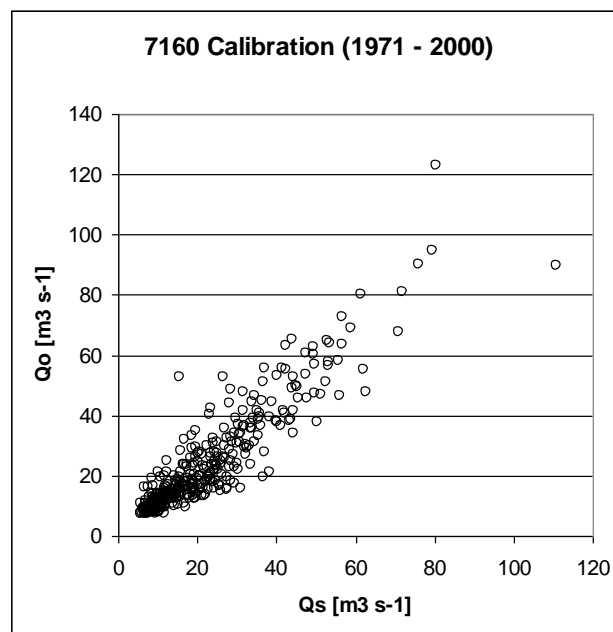


Figure 3.13. Relationship between simulated ( $Q_s$ ) and observed ( $Q_o$ ) mean monthly discharges at the Hron – Banská Bystrica gauging station for the calibration period 1971-2000

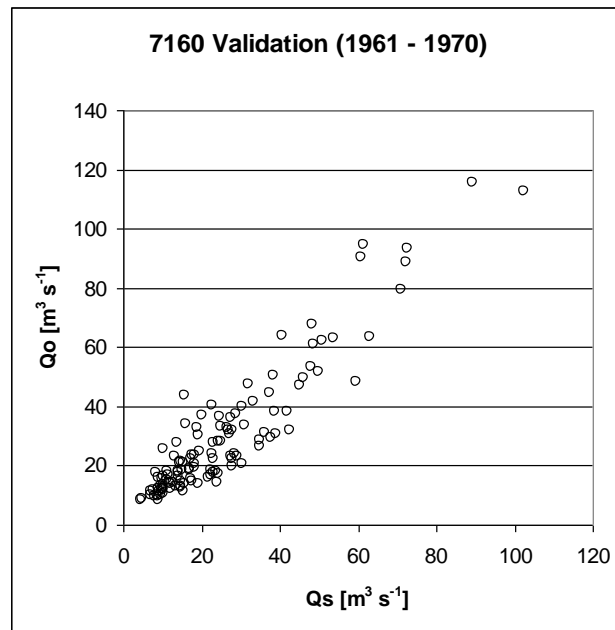


Figure 3.14. Relationship between  $Q_s$  and observed  $Q_o$  mean monthly discharges at the Hron – Banská Bystrica gauging station for the validation period 1961-1970

Table 3.5 Model parameters for the Hron – Banská Bystrica sub-basin

eps	2.185
alpha	1.44
Smax	225
Zinitial	0.994
$T_l$	4.924
$T_s$	-4.983
gamma	1.798
PeffPar	0.866
ActEpar	0.968
Rb	0.089
Drc	0.006

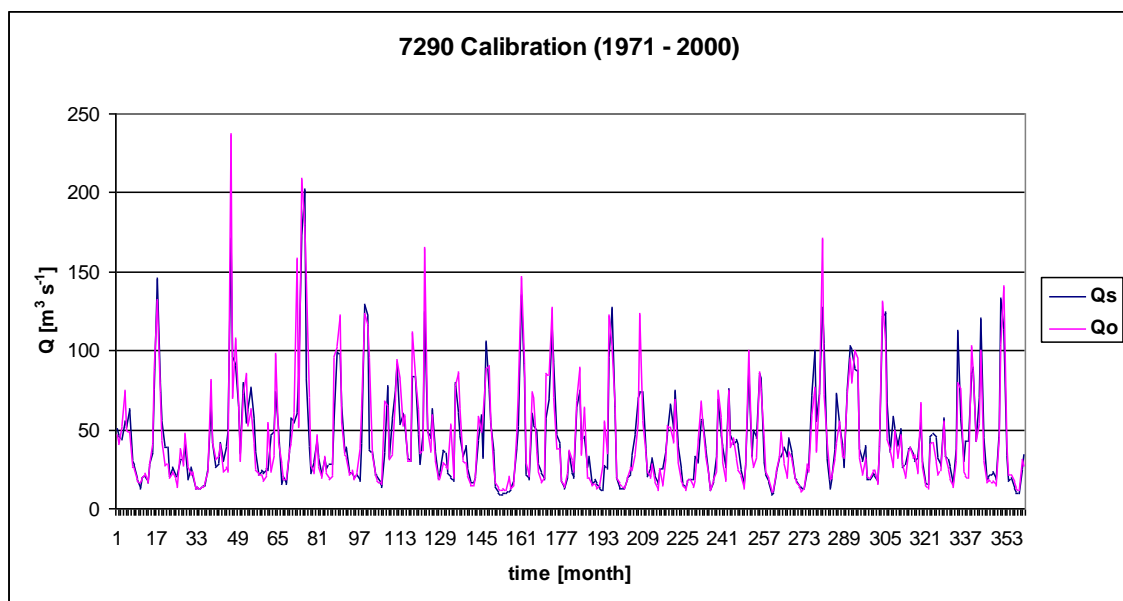


Figure 3.15. Comparison of simulated ( $Q_s$ ) and observed ( $Q_o$ ) mean monthly discharges at the Hron – Brehy gauging station for the calibration period 1971-2000

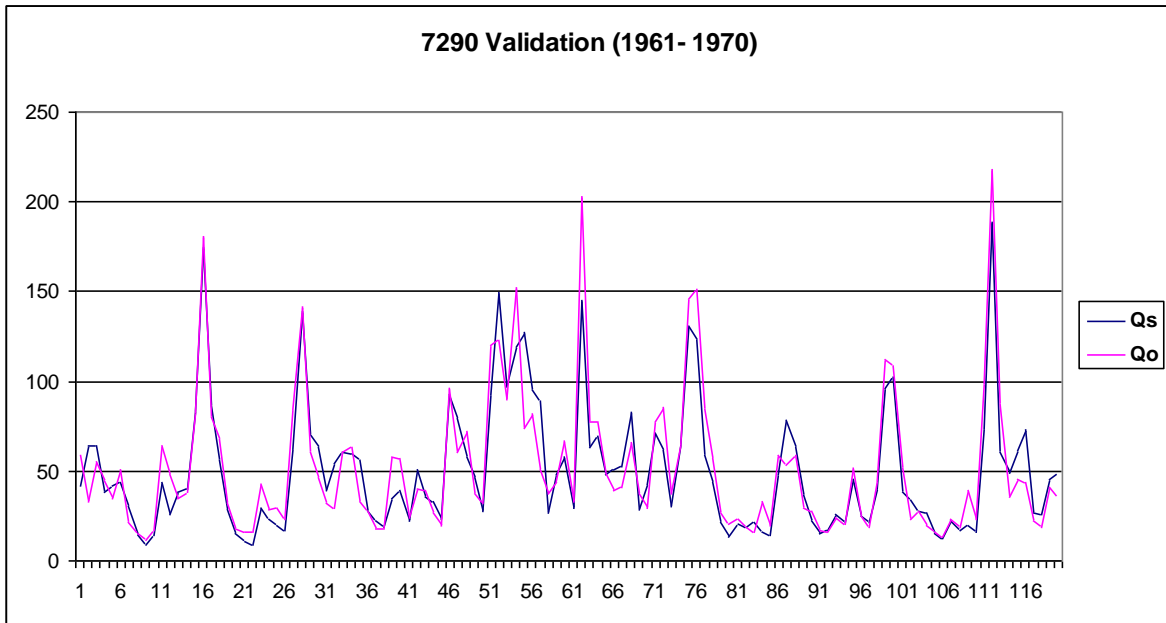


Figure 3.16. Comparison of simulated ( $Q_s$ ) and observed ( $Q_o$ ) mean monthly discharges at the Hron – Brehy gauging station for the validation period 1961-1970

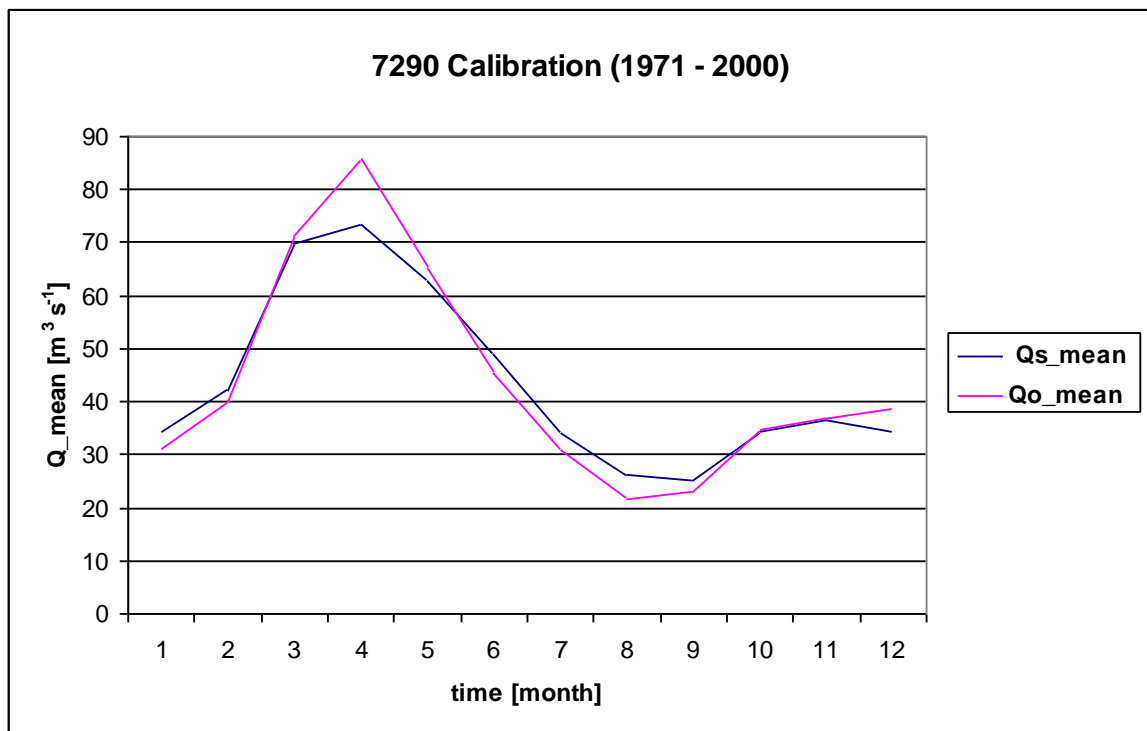


Figure 3.17. Comparison of simulated ( $Q_{s\_mean}$ ) and observed ( $Q_{o\_mean}$ ) long-term mean monthly discharges at the Hron – Brehy gauging station for the calibration period 1971-2000

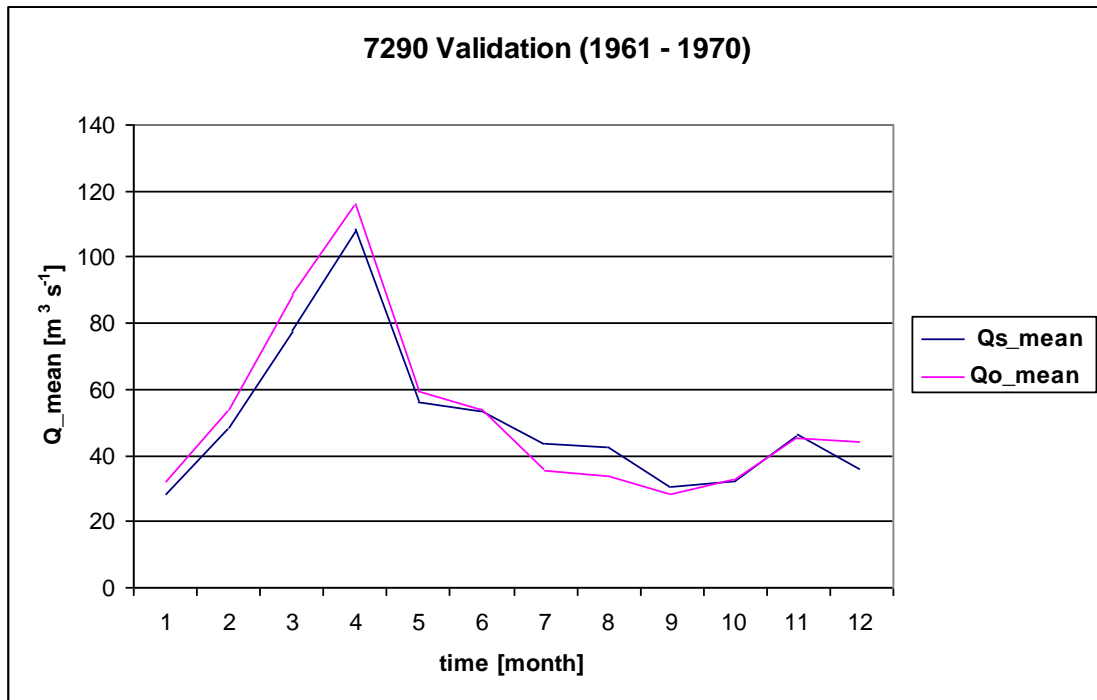


Figure 3.18. Comparison of simulated ( $Qs\_mean$ ) and observed ( $Qo\_mean$ ) long-term mean monthly discharges at the Hron – Brehy gauging station for the validation period 1961-1970

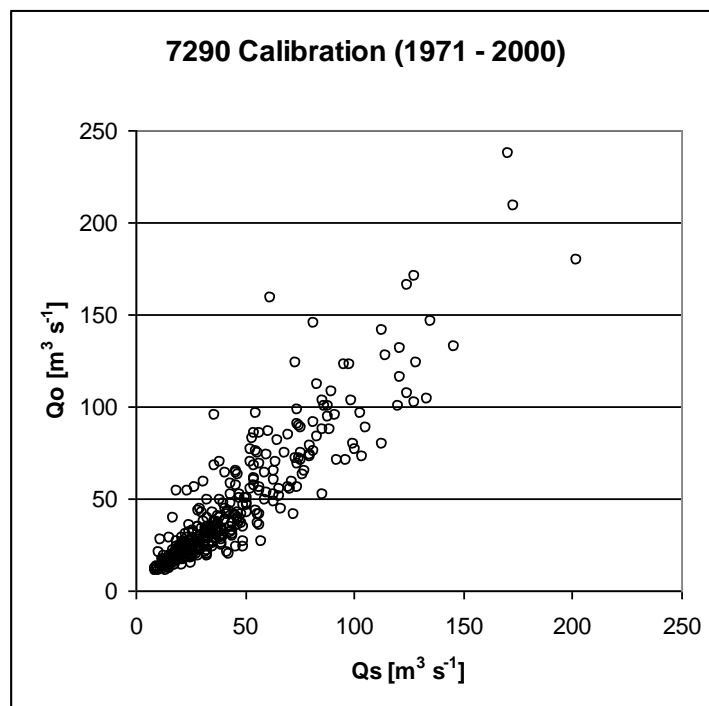


Figure 3.19. Relationship between simulated ( $Qs$ ) and observed ( $Qo$ ) mean monthly discharges at the Hron – Brehy gauging station for the calibration period 1971-2000

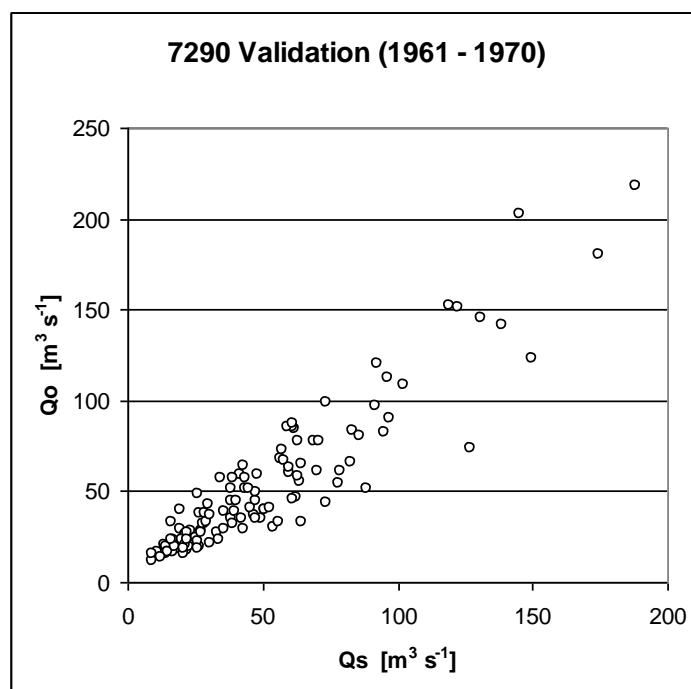


Figure 3.20. Relationship between simulated ( $Q_s$ ) and observed ( $Q_o$ ) mean monthly discharges at the Hron – Brehy gauging station for the validation period 1961-1970

Table 3.6 Model parameters for the Hron – Brehy sub-basin

eps	5.011
alpha	0.973
Smax	255
Zinitial	0.988
$T_1$	4.932
$T_s$	-4.56
gamma	3.106
PeffPar	0.486
ActEpar	2.34
Rb	0.144
Drc	0.027

### 3.5. References

- Danihlík, R. - Hlavčová, K. - Kohnová, S. - Parajka, J. - Szolgay, J. (2004) Scenarios of the change in the mean annual and monthly runoff in the Hron Basin. *J. Hydrol. Hydromech.*, 52, 2004, 4, 291-302.
- Doorenbos J. - Pruitt W.O. (1977) *Guidelines for Predicting Crop Water Requirements*. FAO Irrigation and Drainage, Paper No. 24. FAO, Rome.
- Hlavčová, K. – Kalaš, M. – Szolgay, J. (2002) Impact of climate change on the seasonal distribution of runoff in Slovakia. *Slovak Journal of Civil Engineering*, X, 2, 10–17.
- Novák V. (1995) *Evaporation of water in the nature and methods of its estimation*. Science, SAS Bratislava, 253 pp.
- Szolgay, J. – Hlavčová, K. – Kalaš, M. (2002) Estimation of climate change impact on runoff regime. *Journal of Hydrology and Hydromechanics*, 50, 4, 341–371.
- Szolgay, J. – Hlavčová, K. – Lapin, M. - Danihlík R. (2003) Impact of climate change on mean monthly runoff in Slovakia. *Meteorological Journal*, 6, 3, 9–21.
- Tomlain, J. – Damborská, I. (1999) *Physics of the border layer of atmosphere*. MFF UK, Bratislava, Bratislava, 132 pp.
- Thornthwaite C. W. (1948) An approach toward a rational classification of climate. *Geograph. Rew.* 38, 55-94.

## 4. Buzău and Ialomița river basins (Romania)

### 4.1. Calibration of the rainfall-runoff model WatBal

For studying the impact of a potentially altered climate on runoff from analysed river basins, Buzău and Ialomița, have used WatBal model (Gleick, 1987, Kaczmarek, 1993; Yates, 1994) for the simulation of the runoff in 17 cross-sections (Figure 4.1) on the period 1971-2000. The model has two main modelling components. The first is the water balance component, that uses continuous functions to describe water movement into and out of a conceptualized basin and the second is the component, which allow the compute of the potential evapotranspiration using the Priestly-Taylor radiation approach.

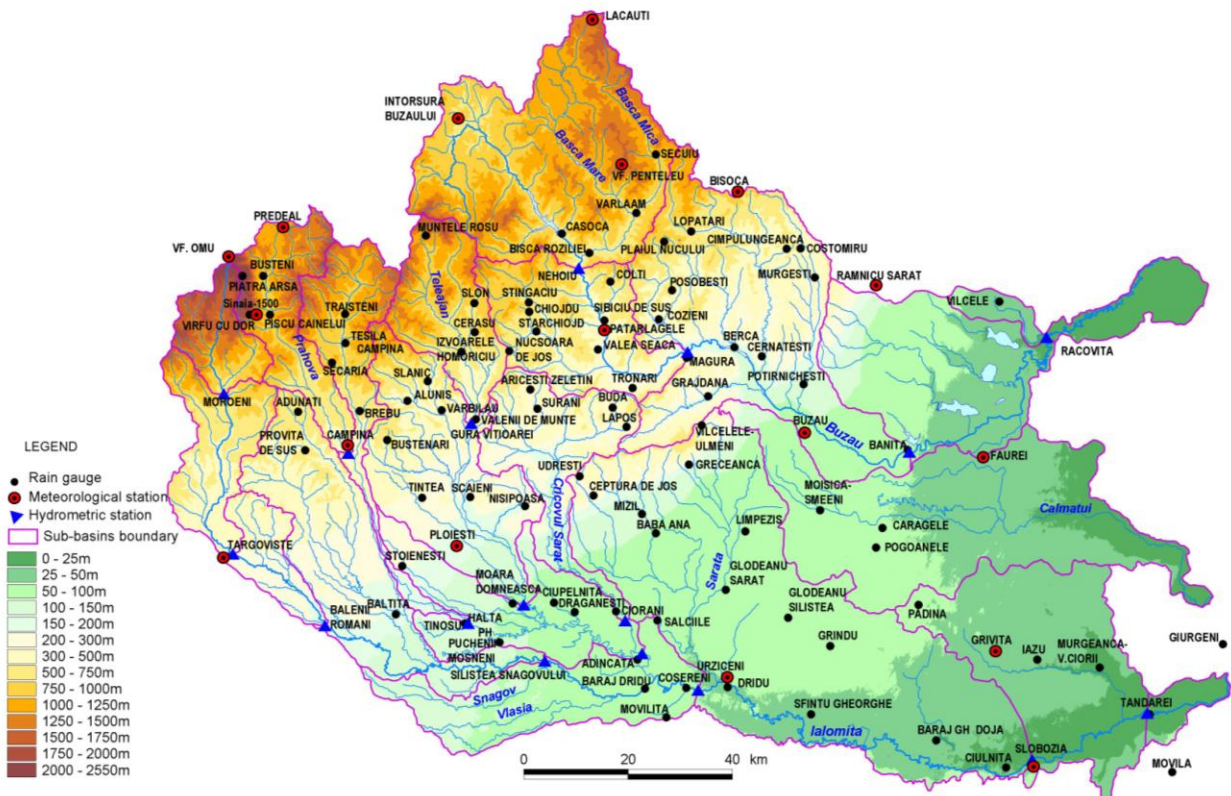


Figure 4.1. Cross-sections selected for applying WatBal model in the river basins Buzău and Ialomița

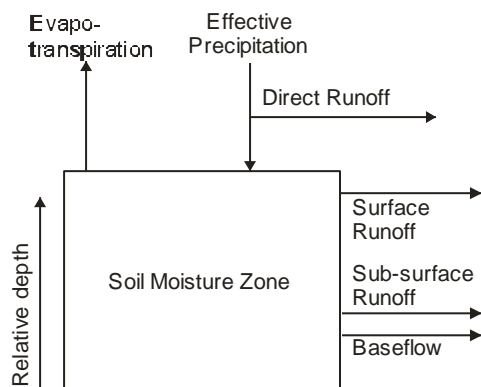


Figure 4.2. Conceptualization the water balance for the WatBal model

The uniqueness of this lumped conceptual model to represent water balance is the use of continuous functions of relative storage to represent surface outflow, sub-surface outflow and evapotranspiration. The water balance component of the WatBal model (Yates, 1994) contains some parameters related to (Figure 4.2): direct runoff ( $\beta$ ); surface runoff ( $\epsilon$ ); sub-surface runoff ( $\alpha$  and  $\gamma$ ); maximum catchment water-holding capacity (field capacity) ( $S_{max}$ ) and base flow ( $Q_b$ ).

Because of the differential approach of the model, varying time steps can be used depending on

data availability and basin characteristics. For larger basins with long times to concentration, longer time steps are recommended. Accordingly for the analysed river basins was used monthly time step.

For the computation of effective precipitation in periods where snowmelt makes up a substantial portion of the runoff water, a temperature index model was used with the upper ( $3^{\circ}\text{C}$ ) and lower ( $-3^{\circ}\text{C}$ ) temperature bounds defined by “trial and error” method.

Evapotranspiration is a function of Potential Evapotranspiration (PET) and the relative catchment storage state.

Potential evapotranspiration is modelled using the Priestly-Taylor method. This method was chosen due to its simplicity and the evidence supporting such an empirical relationship. The Priestly-Taylor method is a radiation-based approach to modelling PET, where the net radiation is computed based on analytical methods. The albedo, a measure of surface reflectivity incorporated into the computation of net radiation, was computed based on the soil moisture content of the soil as well as the predominant surface cover (grass or forest, snow, and fraction of bare ground).

In the WatBal model runoff from impervious surfaces (direct runoff) is controlled by means of  $\beta$  coefficient. The value of this parameter is estimated based on basin characteristics like urbanization and development. Its value should probably be no greater than 0.15 or 15%. In this study was considered  $\beta = 0$ .

Surface runoff is described in terms of the water storage state in soil,  $z$ , the effective precipitation and the base flow, having like parameter  $\varepsilon$  coefficient. Larger values of  $\varepsilon$  correspond to the situation in which the water storage in soil becomes very small, so that the surface runoff tends to zero,  $\varepsilon$  coefficient should not grow much larger than 5.

Sub-surface runoff is a function of the relative storage state times a coefficient,  $\alpha$ . Larger values of this coefficient correspond to an increase of the sub-surface runoff. In most cases, the value of the power term on sub-surface runoff,  $\gamma$ , is 2.0, value which was considered and in the case of applying WatBal model in the analysed river basins, Buzău and Ialomița. However, it was observed that for some river basins it appears that this value is smaller than 2.0. As  $\gamma$  approaches 1.0 the sub-surface runoff responds more linearly with relative storage, indicating a decrease in the holding or retention capacity of the soil. A value of  $\gamma$  less than 2.0 might be, generally, for gravel dominated river basins.

Another model parameter is the maximum catchment holding capacity,  $S_{max}$ . Referring to *Figure 4.2*,  $S_{max}$  is defined as the maximum storage volume, so when  $S_{max}$  is multiplied by  $z$ , the current storage volume for the period is given. The storage variable,  $z$ , is given as the relative water storage state ( $0 \leq z \leq 1$ ). The  $S_{max}$  parameter will likely range between 150 and 700 mm.

The initial storage  $Z_i$  has been determined during the calibration process by comparison for the first month of the simulated discharge hydrograph with the measured one. If the modelled discharge was less than the observed, was re-estimating the initial storage by increasing its magnitude. For example if for  $Z_i = 0.5$  was produces a first months discharge of 1.5 mm/day and the observed was 2.8 mm/day then was increase the relative storage to  $Z_i = 0.75$  and was recalibrate the model. Was repeating this procedure until the simulated discharge was close to the measured value. Because  $Z_i$  is the relative storage, its value must range between 0 and 1.0.

The base flow, in this study, has been estimated as approximately 95% low flow.

The parameters of the WatBal model was calibrated using a unconstrained heuristic algorithm which finds an optimal set of model parameters while meeting the criteria of minimizing the root mean square error between the measured and simulated monthly runoff value. The direct runoff coefficient,  $\beta$ , and the power term on sub-surface runoff,  $\gamma$ , are not part of the optimisation routine.

Time series inputs in the WatBal model need for the calibration of the parameters of this model in the river basins Buzău and Ialomița include: precipitation, temperature and relative air humidity, sunshine hours, wind speed and discharges in the analysed cross-sections.

For the computation of the monthly precipitation on each sub-basin corresponding to the 17 cross-sections have been used values registered at the 18 meteorological stations and 89 pluviometrical stations.

For the determination of the mean monthly values of temperature, relative air humidity, sunshine hours and wind speed on each analysed sub-basins have been used values registered at the 18 meteorological stations.

Note that for the period with missing observations, from some meteorological stations, the values was have been determined on the basis of some correlations using the values from proximate meteorological stations from respective point.

## 4.2. Calibration of WatBal model paramiters

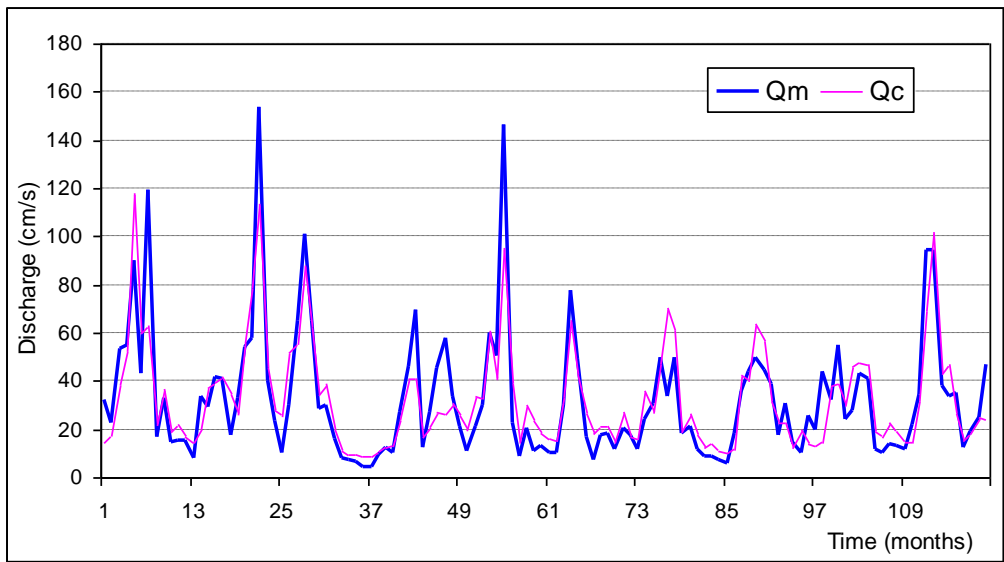
Using inputs data and initial values of the parameters of the WatBal model was simulated mean monthly discharge hydrographs for the river basins Buzău and Ialomița in 17 cross-sections.

The optimum values of the parameters of the WatBal model for the cross-sections considered in the river basins Buzău and Ialomița are presented in the *Table 4.1*.

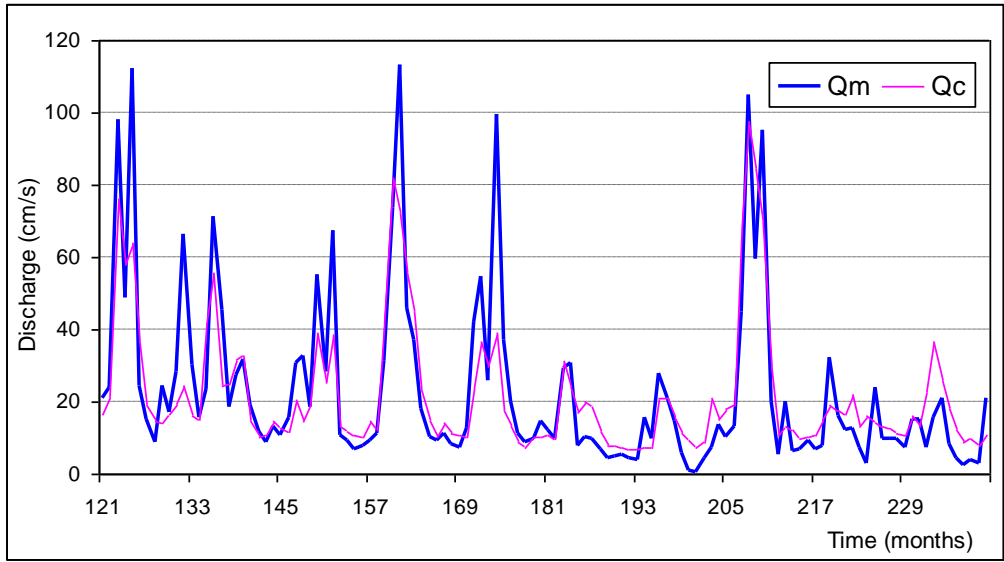
*Table 4.1. Calibration values of the WatBal model parameters*

<i>River basin</i>	<i>River</i>	<i>Cross- section</i>	$Z_i$	$Q_b$ (mm/zi)	$S_{max}$ (mm)	$\beta$	$\varepsilon$	$\alpha$	$\gamma$
Buzău	Buzău	Nehoiu	0.34	0.289	350	0	0.73	7.96	2
		Măgura	0.49	0.233	335	0	1.25	2.83	2
		Banița	0.44	0.139	400	0	1.89	1.0	2
		Racovița	0.37	0.089	455	0	2.32	0.98	2
Ialomița	Ialomița	Moroeni	0.57	0.365	395	0.28	1.64	2.01	2
		Târgoviște	0.63	0.170	420	0	2.15	0.4	2
		Bălenii Români	0.59	0.107	580	0	3.14	0.22	2
		Siliștea Snagovului	0.74	0.059	685	0	6.28	0.43	2
	Prahova	Adâncata	0.59	0.239	475	0	2.60	0.51	2
		Câmpina	0.51	0.459	420	0	1.67	4.53	2
		Halta Prahova	0.67	0.333	395	0	1.80	1.0	2
	Teleajen	Gura Vitioarei	0.64	0.082	400	0	1.61	3.20	2
		Moara Domnească	0.65	0.264	405	0	2.80	0.54	2
	Cricovul Sărat	Ciorani	0.59	0.052	660	0	3.22	0.04	2
	Ialomița	Coșereni	0.54	0.153	460	0	2.45	0.52	2
		Slobozia	0.57	0.106	580	0	3.70	0.50	2
		Țândărei	0.35	0.101	605	0	3.0	0.5	2

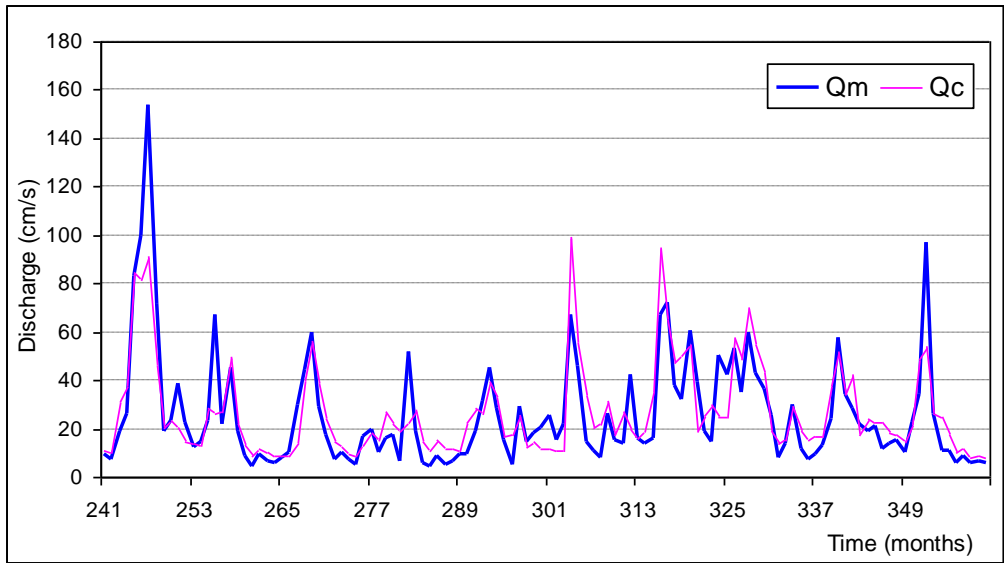
As example, in *Figures 4.3a,b,c* and *Figures 4.4a,b,c* the mean monthly discharge hydrographs for the period 1971-2000 at the hydrometric station Racovita on the Buzău River and at the hydrometric station Tândărei on the Ialomița River, respectively, are presented. These hydrometric stations are situated near the outlets.



(a) 1971 – 1980 period

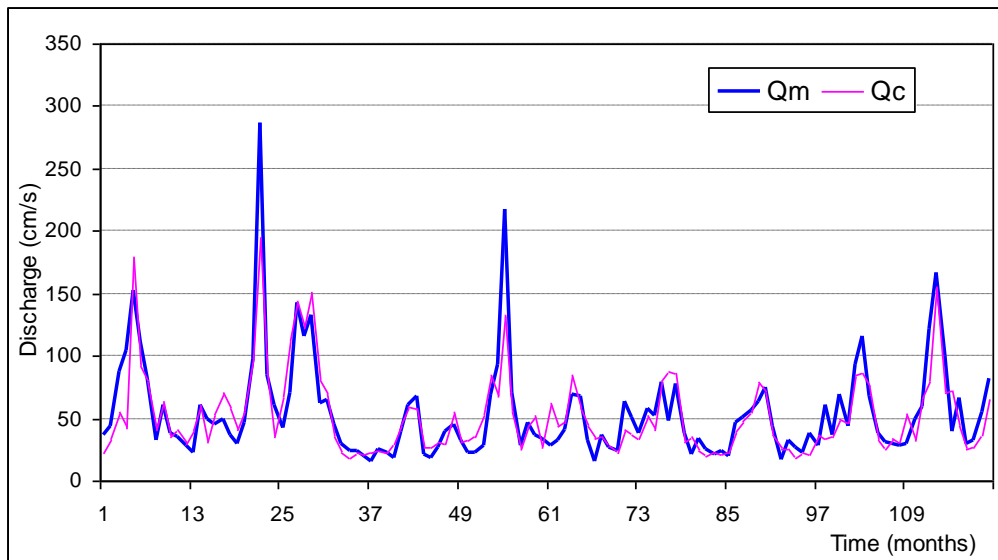


(b) 1981 – 1990 period

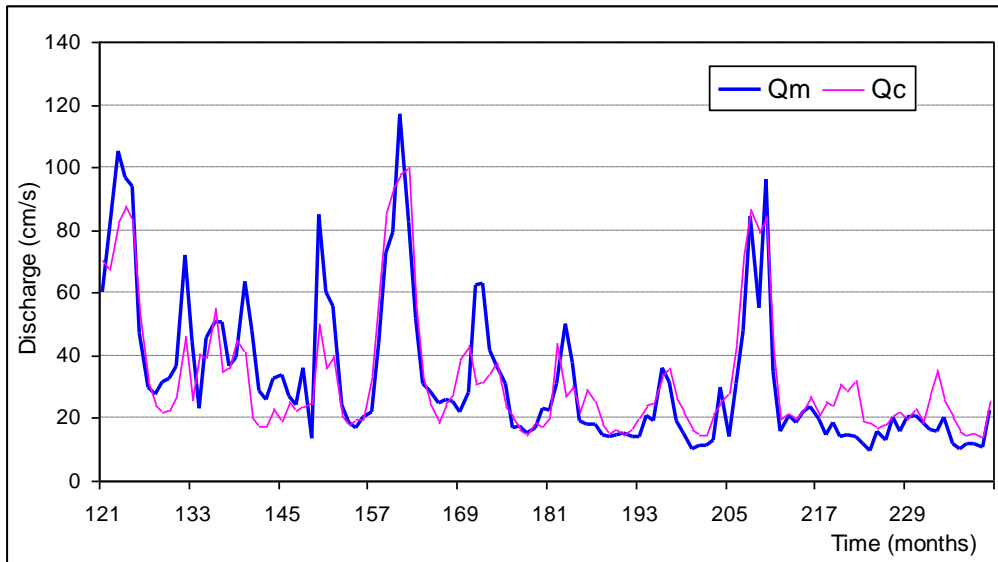


(c) 1991 – 2000 period

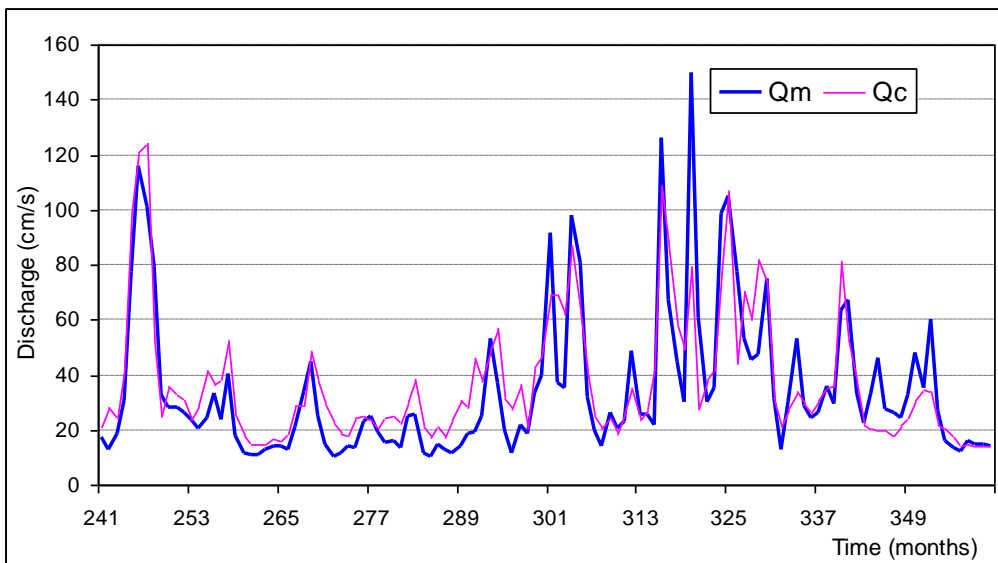
Figure 4.3. Measured ( $Q_m$ ) and simulated ( $Q_c$ ) mean monthly discharge hydrographs in the period 1971 - 2000 at the hydrometric station Racovița on the Buzău River



(a) 1971 – 1980 period



(b) 1981 – 1990 period



(c) 1991 – 2000 period

Figure 4.4. Measured ( $Q_m$ ) and simulated ( $Q_c$ ) mean monthly discharge hydrographs in the period 1971 - 2000 at the hydrometric station Țândărei on the Ialomița River

The errors between the measured and simulated discharges using WatBal model was estimated by means of the following numerical criteria:

- The root mean square error (*RMSE*):

$$RMSE = \sqrt{\frac{F}{N}} \quad (4.1)$$

$$\text{with: } F = \sum_{i=1}^N (O_i - \hat{O}_i)^2 \quad (4.2)$$

where:  $O_i$  are the measured discharges;  $\hat{O}_i$  - the simulated discharges;  $F$  - the residual variation;  $N$  - the number of values of the discharges.

The *RMSE* criterion is dimensional and depends on the length of the series.

- The *NTD* criterion:

$$NTD = 1 - \frac{F}{F_0} \quad (4.3)$$

where the initial variance is calculated with the relation:

$$F_0 = \sum_{i=1}^N (O_i - \bar{O})^2 \quad (4.4)$$

where:  $\bar{O}$  is the mean of the measured discharges.

Nash and Sutcliffe established this criterion, which compares the residual variance with initial one, because they wanted a universal criterion, which not depend on the value of the data and on the length of the series.

The *NTD* criterion tries to compare the forecast errors with the errors produced in the absence of the model, this meaning when the only one forecast that can be elaborated is the mean values of the considered variable. This criterion may give and negative values in the situation in which the simulated values are too far beside measured ones than its average.

The numerical criteria can be presented in the tabular or graphical form. For exemplification, the numerical criteria enumerated above, applied for the period 1971 – 2000, are presented in *Table 4.2* for the all analysed cross-sections.

*Table 4.2. The values of the criteria of estimating the errors between the discharges, in the period 1971 – 2000, for the considered cross-sections on the river basins Buzău and Ialomița*

<i>River basin</i>	<i>River</i>	<i>Cross-section</i>	<i>RMSE</i> ( $m^3/s$ )	<i>NTD</i>
Buzău	Buzău	Nehoiu	9.94	0.66
		Măgura	10.19	0.76
		Banița	11.67	0.74
		Racovița	12.97	0.73
Ialomița	Ialomița	Moroeni	2.76	0.58
		Târgoviște	3.57	0.73
		Bălenii Români	4.21	0.73
		Siliștea Snagovului	4.97	0.77
	Prahova	Adâncata	8.49	0.79
		Câmpina	2.42	0.79
		Halta Prahova	4.37	0.72
	Teleajen	Gura Vitioarei	2.49	0.67
		Moara Domnească	3.49	0.75
	Cricovul Sărat	Ciorani	1.0	0.73
	Ialomița	Coșereni	15.63	0.76
		Slobozia	15.97	0.75
		Țândărei	15.43	0.77

### 4.3. Conclusion

The parameters of the WatBal model were calibrated by simulation of the runoff in 17 cross-sections from river basins Buzău and Ialomița. The acquired results show that the model behaves fairly well given its simplicity.

WatBal model proved to be very sensitive to the definition of effective precipitation, where 1-2 degree variation can be significant in the representation of snow melt, which is used to derive effective precipitation. Also, representation of the melting rate produces a significantly different runoff regime as represented by changes in model parameters. A likely weakness of a lumped approach such as that used in WatBal is the inadequate representation of seasonal variability in the soil moisture holding capacity. Spring runoff occurs over predominantly frozen soils, which has less holding capacity than the dryer summer soils. For the WatBal model, a single maximum holding capacity is specified, so in order to simulate the high spring discharge, a smaller soil moisture capacity value must be given at the expense of high summer runoffs. Although the lumped model parameters lose some of their physical meaning, it is possible to achieve similar calibration results with significantly different calibration parameters. A large soil moisture holding capacity ( $S_{\max}$ ), combined with a large value for the sub-surface flow parameter,  $\alpha$ , will give similar results to a smaller values of these parameters. When larger precipitation changes are prescribed, then the smaller values of  $S_{\max}$  will give substantially more discharge due to the non-linearity.

Therefore, the strong seasonal variation in runoff in the analysed river basins points to the need for possible seasonal parameters within WatBal. However, may assume that these empirically based models, which have been regionally developed and calibrated, can give superior results over a physically based model, which might eliminate the need for additional model parameters.

WatBal model performed well on a monthly time step especially where precipitation was relatively uniform over the year (snowmelt processes were not important) and dramatic runoff changes were largely attributable to evapotranspiration.

### 4.4. References

- Gleick P. H. (1987) The Development and Testing of a Water Balance Model for Climate Impact Assessment: Modeling the Sacramento Basin. *Water Resources Research*, 23(6): 1049-1061
- Kaczmarek Z. (1993) Water Balance Model for Climate Impact Analysis. *ACTA Geophysica Polonica*, v. 41, no. 4, 1-16
- Yates D. (1994) WatBal – An Integrated Water Balance Model for Climate Impact Assessment of River Basin Runoff. IIASA Working Paper, WP-94-64, Laxenburg, Austria